Tail Risk and Equity Risk Premia *

Lai Xu†

Job Market Paper

January, 2014

Abstract

This paper develops a new semi-parametric estimation method based on an extended ICAPM dynamic model incorporating jump tails. The model allows for time-varying, asymmetric jump size distributions and a self-exciting jump intensity process while avoiding commonly used but restrictive affine assumptions on the relationship between jump intensity and volatility. The estimated model implies that the average annual jump risk premium is 6.75%. The model-implied jump risk premium also has strong explanatory power for short-to-medium run aggregate market returns. Empirically, I present new estimates of the model based equity risk premia of so-called "Small-Big", "Value-Growth" and "Winners-Losers" portfolios. Further, I find that they are all time-varying and all crashed in the 2008 financial crisis. Additionally, both the jump and volatility components of equity risk premia are especially important for the "Winners-Losers" portfolio.

*I benefited from discussions with my advisors Tim Bollerslev, George Tauchen, Hao Zhou, and Andrew Patton. I am also grateful for comments from Jia Li, Viktor Todorov and doctoral students in the Duke Financial Econometrics lunch group. All errors are my own. For an updated version of this paper, please check my personal website `http://laixu.me`.

†Department of Economics, Duke University, Durham NC 27708 USA, Email lai.xu@duke.edu, Phone 919-257-0059.

1 Introduction

The equity risk premium—the expected return of the equity market in excess of the risk-free rate—is intimately linked with the equity's risk exposure: intuitively, the higher the equity's riskiness, the higher the risk premium should be to compensate. To study the temporal variation in this risk premium, researchers have recently decomposed it into two components: jump tail risk and diffusive risk. This separation reveals investors' different perceptions of the likelihood of infrequent large jumps and continuous diffusive movements. However, it remains an open question as to how important the time-varying jump behavior in asset prices is for overall risk compensation. This paper attempts to shed light on this issue by proposing a novel semi-parametric estimation method for the time series of both the jump and the volatility risk premia.

The contribution of this paper is threefold. First, I present a novel dynamic model for rare jumps which relaxes several restrictions used in previous studies. The model features a self-exciting process for the jump intensity (also known as the jump arrival rate) and allows the jump shape to be asymmetric and time-varying. This generalizes a standard compound Poisson process specification, which implies independent and identically distributed (iid) increments of jumps as well as strong restrictions for the dynamics of the jump intensity.[1] A self-exciting jump intensity allows for jumps that are not only path-dependent (in that jumps are clustering over time), but also allows past jumps to influence the arrival rate of the future jumps.[2] The distribution of the jump size is commonly assumed to be time-invariant and typically Gaussian. I also relax this stringent assumption and allow for Frechet-type distributions, thereby nesting a large class of (possibly asymmetric) distributions.[3]

Second, I derive closed-form solutions for the jump and volatility components of the equity risk premium in a stylized intertemporal capital asset pricing model (ICAPM). In contrast to a recent work by Campbell et al. (2013), my model is cast in continuous-time with more empirically realistic jumps. The endogenously determined jump component of the equity risk premium entails a multi-factor structure that is directly related to the jumps in total wealth. As usual, this premium can also be conveniently expressed

[1] For example, Maheu et al. (2013) assume that the jump intensity follows an auto-regressive model and exposed to independent diffusive shocks.

[2] One of Eraker's earlier work Eraker (2004) sheds some light on the self-exciting jump intensity model by assuming the volatility co-jumps with the asset price, and the jump intensity inherits the same feature from a linear relationship with the volatility. A working paper by Aït-Sahalia et al. (2013) uses the mutually exciting processes in the international equity markets. But in their model, the volatility is independent of the jump intensity. In contrast to these studies, the jump intensity here has a flexible dependence structure with the volatility.

[3] Because of this setting, the model no longer imposes the same decay rate for both positive and negative jumps, potentially manifesting in much richer dynamic properties. The jump shape, characterized by the decay rate, is the key determinant of the jump size distribution. The higher the decay rate, the lower the probability implied for a jump of a given size.

as the difference in ex-ante expectation of jump tails between physical ($\mathbb{P}$) and risk neutral ($\mathbb{Q}$) measures.[4] Under each measure, both the time-varying jump shape and the self-exciting jump intensity carry important nonlinear effects on the jump risk premium. On a theoretical level, the framework implies the existence of a non-negligible stochastic shape premium and stochastic intensity premium. The former is introduced by the dynamic response of the total wealth portfolio to the aggregate market portfolio, and the latter comes from the path-dependent and self-exciting jump intensity. In addition to a succinct expression for the equity risk premium, the model implies a direct relationship between $\mathbb{P}$ and $\mathbb{Q}$-measures which is exploited for estimation.

The estimation method is model-free under the risk neutral measure and semi-parametric under the physical measure.[5] Intuitively, short-maturity and deep out-of-money (OTM) options are mostly affected by jumps, allowing us to separately identify the jump risk from the diffusive risk. Based on these option panels, the jump shape parameter is uniquely non-parametrically identified by measuring the slope of option prices versus their associated moneyness; the jump intensity can then be backed out using knowledge of the jump shape parameter.[6] In contrast, under the physical measure, a similar technique is infeasible due to so-called "peso problems."[7] To overcome this difficulty, I exploit the model-implied relationship between the two probability measures. In particular, the symmetric dynamic response of total wealth return identifies the shape premium through the difference between deep OTM puts and OTM calls (after some adjustment). Based on this along with high-frequency intra-day index prices, I estimate the intensity premium without any dynamic restriction.

In the third place, a number of results emerge from the estimated time-series of equity risk premia. Firstly, the jump part of the equity risk premium (ERPJ) has a mean of 6.75% on an annual basis, accounting for 93% of the total risk premium. This number is much higher than earlier estimates by Eraker (2004) and Broadie et al. (2007), but is comparable to the jump risk premium reported in Bollerslev and Todorov (2011b). This larger compensation for rare events is mainly induced by the self-excitation of the jump intensity. Secondly, the serial dependence in different parts of the equity risk premium is a natural channel

[4]There is another strand of literature on equity risk premium, which does not rely on any specified pricing kernel. The advantage of this approach is that it is potentially model-free. However, because of this, the mechanism of the overall risk measurement and especially the role of the collective investor's preference is unclear.

[5]The model-free approach for both measures can guard against potential mis-specification of the model designs, e.g. Bollerslev and Todorov (2011b) and Du and Kapadia (2012).

[6]For similar studies, see Carr and Wu (2003), Bollerslev and Todorov (2011b), Bollerslev and Todorov (2013).

[7]Even with high-frequency intra-day data, it is very unlikely to observe more than hundreds of "medium-sized" jumps in the entire sample period, not alone for more extremely large jumps.

for explaining their strong return predictability. The deeper-tail of jumps and volatility parts together can explain 6.53% of the total variation of three-month market returns. From one to six months, the associated R^2s stay well above 2.79%. This strong forecastability reflects the importance of considering the special structure of jumps separately from volatility. Based on the estimated beta, the resulting jump and volatility components of the portfolio's equity risk premium deliver strong predictive power for that portfolio returns in short horizons of one-six months. Specifically, the "Winners-Losers" portfolio (WML) is well explained by the deeper-tail of jump and the volatility parts of the WML's equity risk premium with R^2 up to 34.88% at a half-year horizon.

There is a large related literature pertinent to the models used and modified in this paper. The closed-form model solution is similar in form to consumption based models such as "rare-disaster" or "long-run risk." Wachter (2006) uses a jump process to model the disaster events for consumption and she shows that the equity risk premium depends on the time-varying jump risk. Drechsler and Yaron (2011) assume the consumption growth process is smooth, but the volatility of short-run consumption growth is exposed to a jump component which then implies a jump risk premium in the equity market. In contrast to these models, my extended ICAPM postulates that investors take certain types of risk in asset price as given, and then choose their consumption to satisfy the budget constraints, rather than the other way around. Since the goal of this paper is to estimate the equity risk premium, ICAPM conveniently avoids the use of consumption data which is not measured in high enough frequency.

The estimation procedure is related to earlier studies using a variety of jump diffusion models to jointly explain options and the underlying stock price dynamics in a unified framework. These models typically rely on specific parametric assumptions: e.g. Pan (2002) and Eraker (2004) assume that the jump intensity is affine in the stochastic volatility.[8] Santa-Clara and Yan (2010) proposes a more flexible path-dependent jump intensity model to differentiate it from the volatility and argue that jump risk is more important than diffusive risk.[9] A recent paper by Li and Zinna (2013) seeks to estimate a self-exciting dynamic for the jump intensity, while at the same time allowing for volatility jumps.

[8]Most of the options literature estimates a parametric model on options data and then evaluates the fit via model implied asset prices, e.g. Bates (1996), Bates (2000), Bakshi et al. (1997). These studies strictly rely on the stochastic volatility model by Heston (1993) in which the jump intensity is either constant or affine in volatility. Broadie et al. (2007) employs both options and the index price in the estimation; their proposed model allows volatility jump but the jump intensity is constant.

[9]Maheu et al. (2013) uses the asset price only in a much longer time window; they also model the jump intensity separately in addition to a two-factor volatility structure. Both Santa-Clara and Yan (2010) and Maheu et al. (2013) successfully obtain significant equity risk premiums associated with different latent factors.

In studying the time-varying jump shape, one strand of literature uses daily asset returns to show that the power-law parameter may change over time, e.g. Galbraith and Zernov (2004) applies the idea in the equity index, while Kelly (2011) relies on a large cross-section of stock returns. Another strand employs option prices to estimate the parameters of a Generalized Pareto Distribution, e.g. Hamidieh (2012), Vilkov and Xiao (2013). In contrast to the above studies, I only require short-maturity deep out-of-money option panels to estimate the jump shape under both risk neutral and physical measures. This is a benefit of having a model-implied closed-form pricing kernel.

My empirical results contribute to the studies of short-run return predictability. The variance risk premium (the difference between the statistical and risk-neutral expectation of the corresponding forward variation) shows strong return predictability at quarterly horizon, first documented by Bollerslev et al. (2009), further investigated by Drechsler and Yaron (2011), Bollerslev et al. (2011), among others. Following Li and Zinna (2013), the decomposition (volatility and jump parts) of the variance risk premium significantly improves their forecasting power and the degree of this predictability has a hump shape pattern peaking at three months. However, my decomposition is based on a semi-parametric estimation procedure with only short-dated options, while Li and Zinna (2013) require a tightly specified parametric model and information about the term structure of the variance swap rates.

The rest of the paper is organized as follows: Section 2 presents the general setting for asset return process, section 3 shows an extended ICAPM with jumps, section 4 discusses the estimation strategy, section 5 describes the data and estimation results, and section 6 concludes.

2 Asset Return Dynamics

To study the risk premium for the aggregate market and individual equities, I set up a model for the distributional properties of asset returns. This approach is quite general and forms the foundation of the structural model I later present in section 3.

2.1 Rare Jump Diffusion Model

Let $(\Omega, \mathcal{F}, \mathbb{P})$ be a probability space with information flow $(\mathcal{F}_t)_{t>=0}$. On this space, I model the cumulative return on the aggregate equity market R_t as a rare jump diffusion process satisfying,[10]

$$\frac{dR_t}{R_{t^-}} = a_t dt + \sigma_{m,t} dW_{m,t} + \int_{\mathbb{B}} (e^x - 1)\tilde{J}(dt, dx). \tag{2.1}$$

where a_t refers to the instantaneous drift, $\sigma_{m,t}$ is the stochastic volatility, and $W_{m,t}$ denotes a standard Brownian motion. Both a_t and $\sigma_{m,t}$ are locally bounded cad-lag processes and left unspecified at this stage.[11] J is a random measure for counting jumps on $[0, \infty) \times \mathbb{B}$, with a predictable jump compensator (or intensity measure) $v_t(dx)dt$ such that $\int_{\mathbb{B}} v_t(dx)dt < \infty$. $\mathbb{B}$ is defined as a subset of the real line, $\mathbb{B} = [-\infty, -b^-] \bigcup [b^+, +\infty]$, both b^+ and b^- are positive numbers.[12] Consequently, the compensated jump measure $\tilde{J}(dt, dx) = J(dt, dx) - v_t(dx)dt$ is a martingale measure and $\int_{\mathbb{B}}(e^x - 1)\tilde{J}(dt, dx)$ is a martingale process.[13]

In this model, given the information flow $\mathcal{F}_t$, the future return is exposed to two types of shocks: a continuous martingale ($\sigma_{m,t} dW_{m,t}$), and a discontinuous martingale which is the "demeaned" sum of realized large jumps. "Large" jumps refer to extremely rare events, which I take to be the top and bottom quantiles of discontinuous movements. The bounds b^- and b^+ define these threshold quantiles. In section 4, I use option implied volatility to determine numerical values for b; this method generates sufficiently large thresholds to pass any existing jump test.[14] For a more general setup including both large and small jumps based on Poisson random measure, see Jacod and Todorov (2010).

[10] The cumulative return R_t is not the asset price P_t, because R_t contains both capital gains and cash flow, $\frac{dR_t}{R_{t^-}} = \frac{dP_t + D_t dt}{P_{t^-}}$ where D_t is the dividend payout at time t.

[11] In general asset pricing models, such assumptions are widely used, see e.g. Bollerslev and Todorov (2011b). Depending on the properties of total wealth return and the agent's preference, a_t can takes different functional forms in an arbitrage-free world. I provide an endogenous model solution for a_t in section 3.

[12] In the empirical sections, I let both b^+ and b^- to be both time-varying and sufficiently large.

[13] Compared to an infinite activity process, a rare jump diffusion process defines jumps as rare events and these large jumps are of finite variation. Since small jumps with possibly infinite activity are excluded in the current setup, the finite variation condition for a martingale process is naturally satisfied here.

[14] In appendix C, based on Barndorff-Nielsen and Shephard (2004), I test for the jump existence through intra-day high-frequency prices.

2.2 Time-varying Jump Intensity Measure

I model the jump measure $J([0,t] \times \mathbb{B})$ as depending on an underlying counting process N_t which is independent of the jump size. In this underlying process, the number of jumps per unit of time follows a Poisson process, i.e. $dN_t \sim Poisson(\lambda_t dt)$. This leads to a multiplicatively separable intensity measure $v_t(dx)dt = \lambda_t f_t(x)dxdt$, where λ_t is the instantaneous intensity of jump occurrences and $f_t(x)$ is a density function for the jump size. There are two sources of randomness in the intensity measure: the arrival rate λ_t and the density function $f_t(x)$.

To match the empirical observation that jumps are rare but typically cluster in time, I model the intensity λ_t as a stationary, path-dependent, self-exciting process,

$$d\lambda_t = \kappa_\lambda(\mu_\lambda - \lambda_t)dt + \int_{\mathbb{B}} \varphi_\lambda J(dt, dx). \tag{2.2}$$

where $\varphi_\lambda > 0$ for any $x \in \mathbb{B}$. In this specification, the intensity always jumps up when the cumulative return R_t jumps, then mean reverts until the next jump.[15] A self-exciting process differs from a Poisson process by adding a source of temporal variation which is the number of jumps itself. This implies that, in contrast to other models, the discontinuous increments in both the intensity and the returns are no longer independent.[16] It is worth noting that the intensity λ_t is defined freely from the stochastic volatility $\sigma^2_{m,t}$; however, its self-exciting feature does resemble an ARCH effect in volatility.

At the same time, to capture the possibly time-varying distribution of jump sizes, I employ the double-exponential model of Kou and Wang (2002) with parameter α_t to describe the rate of decay,

$$f_t^{\pm}(x) = \alpha_t^{\pm} \pi^{\pm} e^{\alpha_t^{\pm}|k^{*\pm}|} e^{-\alpha_t^{\pm}|x|}. \tag{2.3}$$

where $f_t^{\pm}(x)$ denotes the density function for positive or negative jumps. Here, π^+ denotes the probability of large positive jumps and $\pi^- = 1 - \pi^+$ the probability of large negative jumps. This new source of randomness in the jump distribution has also been investigated by Bollerslev and Todorov (2013); they also use a heavy tail distribution instead of Merton-type normal distribution to accommodate the complex dynamic tail.[17]

[15] The counting process N_t with intensity λ_t as in equation (2.2) is also called a Hawkes process, first used by Hawkes (1971b) and recently adopted by Aït-Sahalia et al. (2013). The only difference between a compound Poisson process and a Hawkes process is the independent increment assumption.

[16] Alternative specifications of the jump intensity are $\lambda_t \propto \sigma^2_{m,t}$ and $\sigma^2_{m,t}$ has no jump component (see Aït-Sahalia et al. (2012)) or that λ_t is a process independent of volatility $\sigma^2_{m,t}$ (see Maheu et al. (2013)).

[17] While Bollerslev and Todorov (2013) focuses on the dynamic features under the risk neutral measure $\mathbb{Q}$, this paper tries to describe shifting jump shapes under both $\mathbb{P}$ and $\mathbb{Q}$ measures. A recent study by Vilkov and Xiao (2013) assumes jump size follows a generalized Pareto distribution.

2.3 Co-jumps

To model portfolio returns, I explicitly allow these returns to co-jump with the aggregate market return and response to the aggregate diffusive shocks,

$$\frac{dR_{i,t}}{R_{i,t}} = a_{i,t}dt + \beta^{\sigma}_{i,t}\sigma_{m,t}dW_{m,t} + \sigma_{i,t}dW_{i,t} + \int_{\mathbb{B}}(e^{\beta^{J}_{i,t}x} - 1)\tilde{J}(dt,dx) + \int_{\mathbb{B}_i}(e^{x_i} - 1)\tilde{J}_i(dt,dx_i). \tag{2.4}$$

where $[W_{m,t}, W_{1,t}...W_{N,t}]$ denotes an $(N+1)\times 1$ vector of mutually independent standard Brownian motions, $\tilde{J}_i$ is the compensated Poisson random measure on $[0,\infty)\times\mathbb{B}_i$ with intensity $\lambda_{i,t}$ and jump size distribution $f_t(x_i)$.

By assumption, the time-variation in beta loadings β^{σ}_i and β^{J}_i comes solely from movements in the jump shape parameters $\alpha^{\mathbb{Q}\pm}_t$,

$$\beta^{J}_{i,t} = \beta^{J\pm}_{i,0} + \frac{\beta^{J\pm}_{i,1}}{\alpha^{\mathbb{Q}\pm}_t}, \qquad \beta^{\sigma}_{i,t} = \beta^{\sigma}_{i,0} + \frac{\beta^{\sigma}_{i,1}}{\alpha^{\mathbb{Q}-}_t}. \tag{2.5}$$

where $\beta^{J\pm}_{i,0}$, $\beta^{J\pm}_{i,1}$, $\beta^{\sigma}_{i,0}$ and $\beta^{\sigma}_{i,1}$ are scalars to measure the risk exposure to jump and diffusive factors. The non-zero loadings $\beta^{J\pm}_{i,1}$ and $\beta^{\sigma}_{i,1}$ imply that the co-movements with the aggregate market will change when the jump shape parameters change.

3 An Inter-temporal Model with Stochastic Volatility and Jumps

To better understand the risk return trade-off and to provide further insight into the estimation of equity risk premia, I extend the endowment economy intertemporal capital asset pricing model (ICAPM) of Campbell et al. (2013) to include both stochastic volatility and rare jumps. In this setting, closed-form solutions for both the pricing kernel and the equity risk premium are possible.

3.1 Preferences

I assume a representative agent who has a claim over a consumption stream C_t in every period. This agent has an Epstein-Zin-Weil utility function,

$$U_t = [(1-e^{-\delta s})C_t^{\frac{1-\gamma}{\theta}} + e^{-\delta s}(E[U_{t+s}^{1-\gamma}]|\mathcal{F}_t)^{\frac{1}{\theta}}]^{\frac{\theta}{1-\gamma}}. \tag{3.1}$$

where δ is time discount rate, γ is the risk aversion, and ψ is the inter-temporal elasticity of the substitution, $\theta = \frac{\gamma-1}{\psi^{-1}-1}$.[18] The agent then maximizes his utility over the lifetime consumption choices, which results in a

[18]This utility function collapses to a power utility when the risk aversion parameter equals the inverse of the inter-temporal elasticity of the substitution $\gamma = \frac{1}{\Psi}$. The discrete-time version of this utility is widely used in the long run risk literature pioneered by Bansal and Yaron (2004), and then extended to an continuous-time setting in Bollerslev et al. (2012).

Stochastic Discount Factor (SDF) that is a linear function of log-consumption lnC_t and the log-return on all invested assets $lnR_{c,t}$,[19]

$$dlnM_t = -\theta\delta dt - \theta\psi^{-1}dlnC_t + (\theta - 1)dlnR_{c,t}. \tag{3.2}$$

To keep the affine nature of the pricing kernel and therefore analytical tractability, I follow Campbell and Shiller (1988), Eraker and Shaliastovich (2008) among others by log-linearizing $lnR_{c,t}$ around $w_t = ln(P_{c,t}/C_t)$, which gives a convenient approximation for $lnR_{c,t}$,[20]

$$dlnR_{c,t} \approx \kappa_0 dt + \kappa_1 dw_t - (1 - \kappa_1)w_t dt + dlnC_t. \tag{3.3}$$

With equations (3.2) and (3.3), I can substitute out the consumption process lnC_t. Define the hedging demand $h_t = k_0 + k_1 w_t$.[21] Then equation (3.2) collapses to the following expression,

$$dlnM_t = -\gamma dlnR_{c,t} + \frac{\theta}{\Psi}\left(dh_t - [\psi\delta - \frac{\kappa_0}{\kappa_1} + \frac{1 - \kappa_1}{\kappa_1}h_t]dt\right). \tag{3.4}$$

The first term in this equation represents endowment risk (a negative shock to the return on consumption $lnR_{c,t}$) as an indicator of "bad times." An asset that provides insurance against the market downturn is valuable and thus carries a lower premium. This is because investors dislike the downside risk and pay more for an asset with hedging features. The second term arises from other types of risks that matter for the pricing kernel. To further investigate this, I construct an explicit rare jump diffusion model for the return on total wealth $R_{c,t}$.

3.2 Return on Consumption and Volatility Dynamics

I consider a rare jump diffusion model for the endowment return on consumption stream C_t in a similar fashion as the return on the aggregate market in equation (2.1)

$$\frac{dR_{c,t}}{R_{c,t^-}} = a_{c,t}dt + \sigma_{c,t}dW_{c,t} + \int_{\mathbb{B}}(e^{\frac{\gamma_{\mu,t}}{\gamma}x} - 1)\tilde{J}(dt, dx) \tag{3.5}$$

$$dq_t = \kappa_q(\mu_q - q_t)dt + \varphi_q\sqrt{q_t}dW_{q,t} \tag{3.6}$$

[19] For a detailed derivation of this formula, see appendix A in Bollerslev et al. (2012). For a discrete time version for the solution, see Campbell (1993).

[20] Engsted et al. (2012) supports the accuracy of the Campbell-Shiller approximation. Here $\kappa_1 = exp(E(w_t))(1 + exp(E(w_t))^{-1}$ and $\kappa_0 = ln[1 + exp(E(w_t)] - \kappa_1 E(w_t)$.

[21] If an equity can hedge against certain state variables, its risk premium will be adjusted accordingly. This is the key element that differentiates ICAPM from CAPM and the fundamental reason for multiple factors model. For example, Campbell et al. (2013) assume the volatility is stochastic and they find that the shock to volatility is one of the state variables that describes the investment opportunity set. Thus any portfolio that is positively correlated with the volatility shock is a hedging portfolio and should earn a lower equity risk premium.

where $\sigma_{c,t}dW_{c,t} = \sigma_c dW_{c^\perp,t} - \varphi_c \sqrt{q_t} dW_{q,t}$, $\sigma^2_{c,t} = \sigma^2_c + \varphi^2_c q_t$, as for the market return $\sigma_{m,t}dW_{m,t} = \sigma_c dW_{c^\perp,t} - \varphi_m \sqrt{q_t} dW_{q,t} + \sigma_m dW_{m^\perp,t}$, $\sigma^2_{m,t} = \sigma^2_c + \varphi^2_m q_t + \sigma^2_m$, $dW_{c^\perp,t}, dW_{m^\perp,t}$ and $dW_{q,t}$ are mutually independent shocks. The volatility component q_t follows a Heston model, or a square root process. This captures the "leverage effect" commonly documented in the literature: volatility goes up when asset price goes down. In fact, this is why volatility is positively priced as a risk factor in the economy.[22]

The last component represents the co-jumps with the market return R_t, with proportionality parameter $\frac{\gamma_{J,t}}{\gamma}$. Previous studies have assumed that $\gamma_{J,t} = \gamma$, i.e. the jump size in total wealth return is the same as the jump size in the aggregate equity market return. In the present setup, despite dependence on a common jump counting process, the total wealth return and the aggregate equity market can have jumps of differing sizes. To capture this, I allow $\gamma_{J,t}$ to be time-varying and different from γ.

The modeling assumptions of the above specifications allow me to study total wealth return and the pricing kernel in a more flexible way, while simultaneously capturing the fact that the aggregate equity market can be more volatile. Based on this configuration, I now study the model implied equity risk premium.

3.3 Decomposition of the Equity Risk Premium

I use a traditional approach found in the long-run risk literature; that is, under a no arbitrage condition, I solve the equity risk premium for the aggregate market return R_t in equation (2.1),

$$a_t = r_{f,t} + \gamma\sigma^2_c + \varphi_m(\gamma\varphi_c + \phi_q)q_t + \lambda_t\left(\int_B (e^x - 1)f_t(x)dx - \int_B (e^x - 1)e^{-\gamma_{J,t}x + \phi_{\lambda,t}} f_t(x)dx\right). \tag{3.7}$$

Defining the instantaneous equity risk premium as the difference between the drift term a_t and the risk free rate $r_{f,t}$, $ERP_t = a_t - r_{f,t}$, the total equity risk premium ERP_t then consists of two components: a volatility part $ERPV_t$ and a jump part $ERPJ_t$,

$$ERP_t = ERPV_t + ERPJ_t, \tag{3.8}$$

$$ERPV_t = \gamma\sigma^2_c + \varphi_m(\gamma\varphi_c + \phi_q)q_t, \tag{3.9}$$

$$ERPJ_t = \lambda_t\left(\int_B (e^x - 1)f_t(x)dx - \int_B (e^x - 1)e^{-\gamma_{J,t}x + \phi_{\lambda,t}} f_t(x)dx\right). \tag{3.10}$$

This decomposition naturally represents different compensation for diffusive and jump risk. If there is no jump $\lambda_t = 0$, the equity risk premium degenerates to $ERPV_t > 0$, where the temporal variation is captured

[22] See appendix A for the price of volatility factor q_t and appendix D for a small calibration study.

by the volatility factor q_t only. However, when jumps exist $\lambda_t > 0$, $ERPJ_t$ is added to the overall equity risk premium. On average, $ERPJ_t$ should be positive and manifest the compensation for downside rare events. This separation becomes more important when the jump intensity λ_t is no longer affine in stochastic volatility q_t, reinforcing the idea of different perceptions toward distinct sources of risk.

There is an important implication for the functional form of the jump size distribution under the risk neutral measure,

$$f_t^{\mathbb{Q}\pm}(x) = \alpha_t^{\mathbb{Q}\pm}\pi_t^{\mathbb{Q}\pm}e^{\alpha_t^{\mathbb{Q}\pm}|k^{*\pm}|}e^{-\alpha_t^{\mathbb{Q}\pm}|x|}. \tag{3.11}$$

where $\alpha_t^{\mathbb{Q}+} = \alpha_t^+ + \gamma_{J,t}$, $\alpha_t^{\mathbb{Q}-} = \alpha_t^- - \gamma_{J,t}$. The probability that any negative jump occurs under the $\mathbb{Q}$ measure is a function of $\gamma_{J,t}$,

$$\pi_t^{\mathbb{Q}-}(\gamma_{J,t}) = \frac{1}{1 + \frac{\pi^+}{\pi^-}e^{-\gamma_{J,t}(k_t^{*+}-k_t^{*-})}\frac{\alpha_t^+\alpha_t^{\mathbb{Q}-}}{\alpha_t^{\mathbb{Q}+}\alpha_t^-}}. \tag{3.12}$$

If the jump size is exponentially distributed under the statistical measure, then it must also be exponentially distributed under the risk neutral measure, with the shape parameter changed by $\gamma_{J,t}$.[23] I hereby define $\gamma_{J,t}$ as the shape premium, the difference between the negative jump shape under the $\mathbb{P}$ and $\mathbb{Q}$ probability measures. This (non-zero) shape premium comes from the dynamic response of total wealth portfolios to jumps in the aggregate market with size adjustment $\gamma_{J,t}/\gamma$. If total wealth return is perfectly diversified and immune to the market jumps $\gamma_{J,t} = 0$, the shape premium will disappear and the $\mathbb{P}$ and $\mathbb{Q}$-measure probabilities of negative jumps are the same $\pi_t^{\mathbb{Q}-} = \pi^-$.

The jump intensity under the $\mathbb{Q}$ measure relates to the $\mathbb{P}$- measure intensity in a different way,

$$\lambda_t^{\mathbb{Q}} = \lambda_t \times e^{\phi_{\lambda,t}}\int_B e^{-\gamma_{J,t}x}f_t(x)dx. \tag{3.13}$$

Empirical results in section 5 suggest that the second part $\int_B e^{-\gamma_{J,t}x}f_t(x)dx$ is larger than one, and not large enough to capture the difference between the two intensities under the different probability measures. Therefore, $\phi_{\lambda,t}$ which is measuring most of this wedge, i.e. $\phi_{\lambda,t} \approx log(\lambda_t^{\mathbb{Q}}) - \log(\lambda_t)$ effectively constitutes the intensity risk premium. In contrast to previous equilibrium models, these two intensities no longer share the same dynamic properties, and more importantly this intensity premium is generated from the self-excitation of the jump intensity λ_t.

For any particular portfolio return i in equation (2.4), under the no arbitrage condition, the portfolio's

[23] Drechsler and Yaron (2011) derive a similar result in a discrete time framework.

equity risk premium $ERP_{i,t}$=$a_{i,t} - r_{f,t}$ also consists of two parts,

$$ERP_{i,t} = ERPV_{i,t} + ERPJ_{i,t}, \tag{3.14}$$

$$ERPV_{i,t} = \beta^{\sigma}_{i,t}\left(\gamma\sigma_c^2 + \varphi_m(\gamma\varphi_c + \phi_q)q_t\right), \tag{3.15}$$

$$ERPJ_{i,t} = \lambda_t\left(\int_B (e^{\beta^J_{i,t}x} - 1)f_t(x)dx - \int_B (e^{\beta^J_{i,t}x} - 1)e^{-\gamma_{J,t}x+\phi_{\lambda,t}}f_t(x)dx\right). \tag{3.16}$$

This solution is comparable with the equity risk premium for the aggregate market in equation (3.8). The portfolio's diffusive risk premium is proportional to that of the aggregate market in a traditional way $ERPV_{i,t} = \beta^{\sigma}_{i,t}ERPV_t$. However, the jump part of the equity risk premium $ERPJ_{i,t}$ is nonlinearly related with $\beta^J_{i,t}$ and market information on the risk premium. Presumably the higher β^J_i, the higher risk compensation for that particular portfolio. I leave further discussion to the empirical results in section 5.

4 Estimation Strategy

This section introduces a new semi-parametric estimation method for the jump shape and the jump intensity. These estimates are essential to construct the jump and the diffusive risk premium. Under the risk-neutral measure, I use a direct and model-free approach based on option data only; under the statistical measure, both options and high-frequency data are needed. Lastly, the resulting jump shape and the jump intensity estimates make it possible to eliminate the jump bias embedded in the VIX index (CBOE), which helps to further reveal the volatility part of the equity risk premium.

4.1 Jump Shape and Jump Intensity under the Risk Neutral Measure

Most studies assume the jump shape is fixed; in contrast, I allow it to change over time. This modeling assumption makes the estimation more challenging when the jump intensity is also time-varying. However, since the jump shape itself describes distributional properties when jumps occur, which is conceptually very different from the jump intensity (jump arrival rate), the robust estimates for both of them are equally important. Together, the jump shape and the jump intensity provide richer information about rare events from different perspectives.

The idea is to estimate the jump shape first and then the jump intensity in a model-free way. One possible model-free strategy, as shown in Bollerslev and Todorov (2011b), is to use short-dated deep out-of-money options. When the expiration date is near, deep out-of-money options are only hedging against extremely

large jumps.

Specifically, under the risk neutral measure, let $O_{t,T}(k)$ be the option price on the aggregate equity market at time t, with maturity date T, strike price K, and log moneyness k= $\log(K/F_{t^-,T})$, where $F_{t^-,T}$ is the futures price with some undetermined future date after T.[24] Following Bollerslev and Todorov (2011b) and Bollerslev and Todorov (2013), as time-to-maturity $\tau \downarrow 0$ ($\tau = T - t$), k$\uparrow +\infty$ for calls and k$\downarrow -\infty$ for puts, the ratio of the option price to the discounted futures price effectively isolates the jump risk,[25]

$$\frac{e^{r_{t,T}} O_{t,T}(k)}{\tau F_t} \quad \xrightarrow{p} \lambda_t^{\mathbb{Q}} \int_{\mathbb{B}} (e^x - e^k)^{\pm} f_t^{\mathbb{Q}}(dx). \tag{4.1}$$

In fact, for any fixed value $\alpha^{\mathbb{Q}\pm}$, when the time-to-maturity τ decreases, the convergence rate will exponentially increase, and this rate will even be exponentially amplified when the moneyness also goes deeper. As such, in this section and the empirical discussion later on, I will ignore any estimation error if the procedure only depends on the equation (4.1).

Since the jump intensity only enters into equation (4.1) in the first order format, for any pair of options with different log moneyness k_1 and k_2, the ratio of these two option prices on the same day doesn't depend on the jump intensity,

$$log \frac{O_{t,T}(k_2)}{O_{t,T}(k_1)} \quad \xrightarrow{p} log \frac{\int_{\mathbb{B}} (e^x - e^{k_2})^{\pm} f_t^{\mathbb{Q}\pm}(x) dx}{\int_{\mathbb{B}} (e^x - e^{k_1})^{\pm} f_t^{\mathbb{Q}\pm}(x) dx}. \tag{4.2}$$

By using the exact specification of $f_t(x)$ in equation (2.3), the right-hand-side variable includes the shape parameter $\alpha_t^{\mathbb{Q}\pm}$ and the moneyness k_1 and k_2 only, which suggests the shape parameter $\alpha_t^{\mathbb{Q}\pm}$ can be consistently estimated through a sufficiently large number of short-deep-OTM option pairs. In particular, assume on any given day s ($t \leq s \leq T_0$), the errors of downward slope (log option price versus log moneyness) are independent with a median zero conditional on $\mathcal{F}_t$. These pricing errors are also independent across different days within a short period of time. Together this suggests a least absolute difference (LAD) estimate for the jump shape,

$$\widehat{\alpha_t^{\mathbb{Q}\pm}} = \underset{\alpha_t^{\mathbb{Q}\pm} \in R}{argmin} \sum_{s=t}^{T-T_0} \sum_{i=2}^{N_s^{\pm}} \left| \frac{log \frac{O_{s,T}(k_{s,i})}{O_{s,T}(k_{s,i-1})}}{k_{s,i} - k_{s,i-1}} - (1 \mp \alpha_t^{\mathbb{Q}\pm}) \right|. \tag{4.3}$$

where $N_s^{\pm}$ is the total number of calls or puts on day s, T_0 is approximately eight calendar days right before the option expires at date T,[26] and the moneyness is sufficiently deep for both calls $k^{\alpha+} < k_{t,1} < k_{t,2} ... < k_{t,N_t^+}$

[24] This is because the only information needed here is the change of the futures price at date t and date T.

[25] See Lemma 1 in Bollerslev and Todorov (2013), in their notation $\phi_t^{\pm} = \lambda_t^{\mathbb{Q}} \alpha_t^{\mathbb{Q}\pm} \pi^{\mathbb{Q}\pm} e^{\alpha_t^{\mathbb{Q}\pm} |k^{*\pm}|}$ with boundary conditions. If $\alpha_t^- > \iota$, $\alpha_t^+ > 3 + \iota$ for some $\iota > 0$, the convergence rate is τ^{ι} and the cumulated return R_t has a finite third moment.

[26] I do not include observations with the maturity shorter than seven days because these options contain large amounts of noise; see discussion in Bollerslev and Todorov (2011b).

and puts $k^{\alpha-} > k_{t,1} > k_{t,2} ... > k_{t,N_t^-}$. This LAD estimator sufficiently down-weights the "outliers" in the minimization problem.[27] In empirical practice, the pooling on a monthly basis ($\tau \leq 35$ days) ensures a large number of option pairs in the estimation.[28]

In light of equation (4.1), the jump intensity under the risk-neutral measure $\lambda_t^{\mathbb{Q}}$ is then identified based on the first-step estimated shape parameter $\alpha_t^{\mathbb{Q}\pm}$ in equation (4.3). Since the model in section 3 implies the same intensity process for both positive and negative jumps, I consequently use both calls and puts to infer the embedded information on the intensity,[29]

$$\widehat{\lambda_t^{\mathbb{Q}}} = \underset{\lambda_t^{\mathbb{Q}} \in R}{argmin} \sum_{s=t}^{T-T_0} \sum_{i=1}^{N_t^-} \sum_{j=1}^{N_t^+} \left| \log \left(\frac{e^{r_{s,T}} CALL_{s,T}(k_{i,s})}{\tau_s F_s} \Big/ \frac{e^{(1-\alpha_t^{\mathbb{Q}+})k_{s,j} + \alpha_t^{\mathbb{Q}+} k_t^{*+}}}{\alpha_t^{\mathbb{Q}+} - 1} + \frac{e^{r_{s,T}} PUT_{s,T}(k_{i,t})}{\tau_s F_s} \Big/ \frac{e^{(1+\alpha_t^{\mathbb{Q}-})k_{s,i} - \alpha_t^{\mathbb{Q}+} k_t^{*-}}}{\alpha_t^{\mathbb{Q}+} + 1} \right) - \log \lambda_t^{\mathbb{Q}} \right|.$$

where k_t^{*+} and k_t^{*-} are the thresholds to define the rare jumps on the real line. Because of the symmetry assumption, the jump intensity has an even larger sample in the estimation.

Together, the estimated asymmetric jump shapes and the symmetric jump intensity provide a full characterization for jumps under the risk neutral measure. They also prove to be helpful for inferring the jump features under the physical measure.

4.2 Jump Shape and Jump Intensity Premiums

The proposed ICAPM in section 3 implies an explicit relation across the two probability measures. Among others, the shape premium $\gamma_{J,t}$, or the difference between the left-jump shape under $\mathbb{P}$ and $\mathbb{Q}$ probability measures, arises from the dynamic response of total wealth to jumps in the aggregate equity market. The higher shape premium is an effect of a larger response.

There are two ways to semi-parametrically estimate the jump shape premium $\gamma_{J,t}$.[30] First, we can use high-frequency prices to estimate the $\mathbb{P}$-measure decay rates, and then compare with their $\mathbb{Q}$-measure decay rates to infer the shape premium $\gamma_{J,t}$. This is only possible if we can observe enough large jumps in the actual prices within a short period of time. In the appendix C, I show that for the entire sample, we can only observe about 347 "medium-sized" jumps. This means the direct use of high-frequency data is infeasible

[27] If one relaxes the independence assumption, he or she can also try to apply the kernel weights for the absolute errors.

[28] Since I eliminate the extremely short to maturity options, $T - T_0 \neq 0$, the workable number of days in one month is 15 instead of 22.

[29] A similar approach is discussed in Bollerslev and Todorov (2013) in their footnote 13. The difference is I use both puts and calls in the estimation to reflect the independence assumption on jump intensity $\lambda_t^{\mathbb{Q}}$ and jump size.

[30] In most of the studies, shape premium $\gamma_{J,t}$ is the same as the time-invariant risk aversion parameter γ. The latter is usually a calibrated number in consumption based asset pricing models to match with the average mean of the aggregate equity risk premium; or it can be estimated in a fully parameterized jump-diffusion model. However, since I am mostly interested in reducing the model assumptions in the estimation, I have no reason to make similar restrictions at this point.

for the shape premium estimation.

The second way (feasible way) is illuminated by the relation between the shape premium and the $\mathbb{Q}$-measure probability in equation (3.12). The intuition behind this approach is the following: given a fixed physical probability for negative jumps (e.g. $\pi^- = 0.5$), the corresponding risk-neutral probability is higher than π if and only if the shape premium $\gamma_{J,t}$ is positive. In other words, $\pi^{\mathbb{Q}-}$ can uniquely identify the shape premium $\gamma_{J,t}$ based on some predetermined $\mathbb{P}$- measure probability and the $\mathbb{Q}$- measure decay rates. To be more specific, by assuming $\pi^+ = \pi^- = 0.5$,[31] it implies that $\pi_t^{\mathbb{Q}-}$ in equation (3.12) is a function of shape parameter $\alpha_t^{\mathbb{Q}\pm}$ and the shape premium $\gamma_{J,t}$ only,

$$\pi_t^{\mathbb{Q}-}(\gamma_{J,t}) \quad = \frac{1}{1+e^{-\gamma_{J,t}(k_t^{*+}-k_t^{*-})\frac{\alpha_t^+\alpha_t^{\mathbb{Q}-}}{\alpha_t^{\mathbb{Q}+}\alpha_t^-}}}. \tag{4.4}$$

Since the probability for negative jumps under the risk-neutral measure $\pi^{\mathbb{Q}-}$ can be estimated by comparing the price of puts and calls, so can the shape premium $\gamma_{J,t}$,

$$\begin{aligned}\widehat{\gamma_{J,t}} = \underset{\gamma_{J,t}\in R}{argmin} \sum_{s=t}^{T-T_0}\sum_{i=1}^{N_s^-}\sum_{j=1}^{N_s^+} \Big| \log\frac{PUT_{s,T}(k_{s,i})}{CALL_{s,T}(k_{s,j})} - (1+\alpha_t^{\mathbb{Q}-})k_{s,i} + (1-\alpha_t^{\mathbb{Q}+})k_{s,j} + \log(\frac{\alpha_t^{\mathbb{Q}-}+1}{\alpha_t^{\mathbb{Q}+}-1}) \\ - \log\left(\frac{\pi_s^{\mathbb{Q}-}(\gamma_{J,t})\ e^{-\alpha_t^{\mathbb{Q}-}k_s^{*-}}}{\left[1-\pi_s^{\mathbb{Q}-}(\gamma_{J,t})\right]\ e^{\alpha_t^{\mathbb{Q}+}k_s^{*+}}}\right)\Big|.\end{aligned} \tag{4.5}$$

where the pricing errors in the put-call pairs are $\mathcal{F}_t-$ independent with a median of zero. As a result, the $\mathbb{P}$-measure shape parameter estimates are $\widehat{\alpha_t^+} = \widehat{\alpha_t^{Q+}} - \widehat{\gamma_{J,t}}$ and $\widehat{\alpha_t^-} = \widehat{\alpha_t^{Q-}} + \widehat{\gamma_{J,t}}$.

This "indirect approach" successfully overcomes the difficulty of estimating the "unobservables." This approach uses a total of $N_s^- \times N_s^+$ observations on each day. In the empirical implementation discussed below, that is approximately 114×15 observations per month. A similar approach can also be applied to the case where $\gamma_{J,t} = \gamma$ by summing the right-hand-side of equation (4.5) over the full sample horizon.

The $\mathbb{P}$-measure jump intensity estimation is complicated by a similar "lack-of-data" problem. In order to make any inference about this "unobserved" jump intensity, I assume a pseudo jump intensity measure exists with a smaller cutoff choice k^{P*+} and k^{P*-}. This means that "medium" and "large" jumps are no longer separable.

[31] From year 1990 to 2011, there are 2644 jumps in total, 1110 are positive jumps (1534 are negative jumps), among which 162 are larger than 0.6% (185 are smaller than -0.6%).

Consider a noisy proxy for the median-to-large jump intensity $E_t JX$,

$$JX^{\pm}_{k_t^{P*\pm},T} \equiv \int_t^T \int_{[k^{P*\pm},\pm\infty]} (e^x - e^{k_t^{P*\pm}}) J(dt,dx), \tag{4.6}$$

$$EJX^{\pm}_{k_t^{P*\pm},T} \equiv E_t JX^{\pm}_{k_t^{P*\pm},T} \xrightarrow{p} \lambda_t \int_{[k^{P*\pm},\pm\infty]} (e^x - e^{k_t^{P*\pm}}) f_t^{\pm}(x)dx. \tag{4.7}$$

The estimated $EJX^{\pm}_{k_t^{P*\pm},T}$ comes from a HAR-VAR Kalman filter approach, and is based on a daily observed vector $Y = [CV, JV^{\pm}, OVER^2, JX^{\pm}]$, where CV is the continuous variation, $JV^{\pm}$ is the left- and right- jump variation, $OVER^2$ is the overnight return squared.[32] Even for medium-sized jumps, on most days $JX^{\pm}_{k_t^{P*\pm},T}$ are both zero, so the variation in $EJX^{\pm}_{k_t^{P*\pm},T}$ mostly comes from the other variables in the vector $Y_{t,T}$.

Together with equation (4.1), I then estimate $\phi_{\lambda,t}$ by taking the log difference of call prices and the right-jump tail EJX_t^+, and the log difference of put prices and the left-jump tail EJX_t^-, for any day $s \in [t, T_0]$,

$$\begin{aligned}\widehat{\phi_{\lambda,t}} = \underset{\phi_{\lambda,t}\in R}{argmin} \sum_{s=t}^{T_0}\sum_{i=1}^{N_s^-}\sum_{j=1}^{N_s^+} |\log\left(\frac{e^{r_{s,T}} CALL_{s,T}(k_{j,s})}{\tau_s F_s \times J\widehat{TX}^+_{[s,T]}} \Big/ \frac{e^{(1-\alpha_t^{\mathbb{Q}+})(k_{s,j}-k_t^{P*+})}}{(\alpha_t^{\mathbb{Q}+}-1)/(\alpha_t^+-1)} + \frac{e^{r_{s,T}} PUT_{s,T}(k_{i,s})}{\tau_s F_s \times J\widehat{TX}^-_{[s,T]}} \Big/ \frac{e^{(1+\alpha_t^{\mathbb{Q}-})(k_{s,i}-k_t^{P*-})}}{(\alpha_t^{\mathbb{Q}+}+1)/(\alpha_t^++1)}\right) \\ - \log\int_{\mathbb{B}} \alpha_t^{\pm} e^{\alpha^{\pm}|k^{*P\pm}|-\gamma_{J,t}x-\alpha_t^{\pm}|x|}dx - \phi_{\lambda,t}|.\end{aligned} \tag{4.8}$$

where the pricing errors are $\mathcal{F}_t-$ independent with a median of zero. Once again, the LAD estimate down-weighs the outliers. As a result, the jump intensity reveals itself naturally as $\widehat{\lambda_t} = \widehat{\lambda_t^{\mathbb{Q}}}/e^{\widehat{\phi_{\lambda,t}}}/\int_{\mathbb{B}} e^{-\widehat{\gamma_{J,t}}x} f_t(x)dx$. In parallel to the shape premium $\gamma_{J,t}$ estimation, this approach also uses a total of $N_s^- \times N_s^+$ observations on each day.

4.3 Jump Part of Equity Risk Premium

The uncovered jump shapes and intensities are building blocks in the construction of the jump risk premium. As stated in the model in section 3, the jump risk premium (or the jump part of the equity risk premium) contains both the risk-neutral and the physical expectation for the rare events, the difference of which justifies the compensated premium. In turn, the jump part of the equity risk premium, or any of its deeper-tails defined on a subset $\mathbb{D} \in \mathbb{B}$, $\mathbb{D} = [-\infty, k_t^{**-}] \bigcup [k_t^{***}, \infty]$, are constructed as below,

$$\widehat{ERPJ}_{\mathbb{D},t} = \widehat{ERPJ}^+_{\mathbb{D},t} + \widehat{ERPJ}^-_{\mathbb{D},t}, \tag{4.9}$$

$$\widehat{ERPJ}^+_{\mathbb{D},t} = \widehat{ERPI}_{\mathbb{D},t} + \widehat{\lambda_t}\int_{\mathbb{D}^+} \widehat{\alpha_t^{\pm}}\pi^{\pm} e^{\widehat{\alpha_t^{\pm}}(|k^{*\pm}|-|x|)+x}dx - \widehat{\lambda_t^{\mathbb{Q}}}\int_{\mathbb{D}^+} \widehat{\alpha_t^{\mathbb{Q}\pm}}\widehat{\pi_t^{\mathbb{Q}\pm}} e^{\widehat{\alpha_t^{\mathbb{Q}\pm}}(|k^{*\pm}|-|x|)+x}dx, \tag{4.10}$$

$$\widehat{ERPJ}^-_{\mathbb{D},t} = \widehat{ERPI}_{\mathbb{D},t} + \widehat{\lambda_t}\int_{\mathbb{D}^-} \widehat{\alpha_t^{\pm}}\pi^{\pm} e^{\widehat{\alpha_t^{\pm}}(|k^{*\pm}|-|x|)+x}dx - \widehat{\lambda_t^{\mathbb{Q}}}\int_{\mathbb{D}^-} \widehat{\alpha_t^{\mathbb{Q}\pm}}\widehat{\pi_t^{\mathbb{Q}\pm}} e^{\widehat{\alpha_t^{\mathbb{Q}\pm}}(|k^{*\pm}|-|x|)+x}dx, \tag{4.11}$$

$$\widehat{ERPI}_{\mathbb{D},t} = -\widehat{\lambda_t}\int_{\mathbb{D}} \widehat{\alpha_t^{\pm}}\pi^{\pm} e^{\widehat{\alpha_t^{\pm}}(|k^{*\pm}|-|x|)}dx + \widehat{\lambda_t^{\mathbb{Q}}}\int_{\mathbb{D}} \widehat{\alpha_t^{\mathbb{Q}\pm}}\widehat{\pi_t^{\mathbb{Q}\pm}} e^{\widehat{\alpha_t^{\mathbb{Q}\pm}}(|k^{*\pm}|-|x|)}dx. \tag{4.12}$$

[32] For details, see section 4.4, and appendix C, for a similar study see Bollerslev and Todorov (2011b).

where if $\mathbb{D} = \mathbb{B}$, $\widehat{ERPI}_{\mathbb{B},t}$ is the difference between the risk-neutral and physical jump intensities $\widehat{ERPI}_{\mathbb{B},t} = -\widehat{\lambda_t} + \widehat{\lambda_t^{\mathbb{Q}}}$.

Compared with a fully parametric model with fixed jump shapes, so that the time-variation of the jump tails only comes from the $\mathbb{P}$- measure jump intensity, I derive a more special structure for the tail risk premium by allowing shifting jump shapes and two distinct jump intensities. Investors will be more richly compensated when the jump shape premium is larger and when the jump intensity is not only path-dependent but also self-exciting.

4.4 Variance Risk Premium

To show the intimate link between the variance risk premium and the volatility part of the equity risk premium, define the quadratic variation of the logarithm market return over $[t, T]$ as,

$$QV_{t,T} \equiv \int_t^T \left(\sigma_c^2 + \sigma_m^2 + \varphi_m^2 q_s\right) ds + \int_t^T \int_B x^2 J(ds, dx). \tag{4.13}$$

Moreover, let $CV_{t,T}$ denote the continuous variation and $JV_{t,T}$ the jump variation,

$$QV_{t,T} = CV_{t,T} + JV_{t,T}, \qquad CV_{t,T} \equiv \int_t^T \left(\sigma_c^2 + \sigma_m^2 + \varphi_m^2 q_s\right) ds, \qquad JV_{t,T} \equiv \int_t^T \int_{\mathbb{B}} x^2 J(ds, dx). \tag{4.14}$$

With this notation, the variance risk premium, or the difference between the $\mathbb{Q}$ and $\mathbb{P}$-measures quadratic variation $QV_{t,T}$ is simply,

$$\begin{aligned} VRP_{t,T} &= E_t^{\mathbb{Q}}[QV_{t,T}] - E_t[QV_{t,T}] \\ &= \underbrace{E_t^{\mathbb{Q}}[CV_{t,T}] - E_t[CV_{t,T}]}_{VRP_{t,T}^{cv}} + \underbrace{E_t^{\mathbb{Q}}[JV_{t,T}] - E_t[JV_{t,T}]}_{VRP_{t,T}^{J}}. \end{aligned} \tag{4.15}$$

The implied variance IV_t quantified by VIX (CBOE), contains a bias from the jump process.[33] Removing the noise from jumps delivers a clean "model-free" measure for the continuous part of the variance risk premium,

$$E_t^{\mathbb{Q}}\widehat{[CV_{t,T}]} = IV_{t,T} - 2\widehat{\lambda_t^{\mathbb{Q}}} \times \int_{\mathbb{B}} (e^x - x - 1)\widehat{f_t^{\mathbb{Q}}(x)} dx, \qquad \widehat{VRP_{t,T}^{cv}} = E_t^{\mathbb{Q}}\widehat{[CV_{t,T}]} - E_t\widehat{[CV_{t,T}]}.$$

The recovered $\widehat{VRP_{t,T}^{cv}}$ contributes to the volatility part of the equity risk premium.[34] In appendix A, I prove that the continuous part of the variance risk premium $VRP_{t,T}^{cv}$ is linearly related to q_t—the driving variable

[33] Implied variance is commonly used in empirical asset pricing studies, see e.g. Bollerslev et al. (2009), Du and Kapadia (2012), among others.

[34] A parametric calibration is needed besides $\widehat{VRP_{t,T}^{cv}}$. See the calibration table in appendix D for details.

for the volatility part of the equity risk premium.[35] In other words, the volatility part of the equity risk premium $ERPV_t$ is affine in the continuous part of the variance risk premium $VRP^{cv}_{t,T}$.

This section discussed a strategic plan to estimate the jump risk premium and the driving variable for the diffusive risk premium. In the next section, I present estimation results and discuss the predictive regressions for short-medium horizon returns.

5 Estimation Results

From the extended ICAPM with stochastic volatility and jumps in section 3, the equity risk premium is naturally decomposed into the jump part and the volatility part. In this section, I apply the estimation strategy in section 4 and present the estimates for the jump shapes and the jump intensities. I also explain the construction of the risk premia for the aggregate market and the different portfolios.

5.1 Data Description

S&P 500 Options

The options on the S&P 500 index are obtained from OptionMetrics. The data sample runs from January 1996 to December 2011, for a total of 4027 trading days. I remove arbitrage observations for both calls and puts based on the mid quotes, moneyness and trading volume.[36]

For each month, I use short-dated and deep out-of-money options (7-45 days time-to-maturity) with the same maturity date to ensure all options contain the information only for a fixed time period. I use deep-out-of-money options to separate jumps from volatility. The "deepness" is defined by the at-the-money Black-Scholes's implied volatility σ_t^{ATM} and time-to-maturity τ; deep-out-of-money calls (puts) are those with log moneyness above (below) $k^{*+} = c^{*+} \times \sigma_t^{ATM} \sqrt{\tau},\ c^{*+} > 0$ ($k^{*-} = -c^{*-} \times \sigma_t^{ATM} \sqrt{\tau},\ c^{*-} > 0$). All together, I have on average 85 "deep" calls per month with $c^{*+} = 1.75$ and 300 "deep" puts per month with $c^{*+} = 2.0$.[37]

S&P 500 High-frequency

The high-frequency intra-day data for the S&P 500 futures are from Tick Data Inc. The data sample runs from January 1990 to December 2011. These prices are recorded every five minutes, with the first observation at

[35] In this setting, the expected continuous variation $E_t^Q[CV_{t,T}]$ and $E_t[CV_{t,T}]$ are also linearly related to q_t, however, the continuous part of the variance risk premium $VRP^{cv}_{t,T}$ is a better choice since it is robust to alternative volatility models, see e.g. the two-volatility structure in Bollerslev et al. (2009).

[36] I apply the standard cleaning rule here; for details see appendix B.

[37] For different choices of the cutoff $k^{*\pm}$, see appendix B. For estimation of $\alpha_t^{\mathbb{Q}\pm}$, I use a higher cutoff for puts to guarantee robust estimates: $k^{\alpha+} = k^{*+}$; $k^{\alpha-} = -3.0 \times \sigma_t^{ATM} \sqrt{\tau} < k^{*-}$.

8:35 (CST) and the last one at 15:00 (CST), for a total of 78 records on each trading day.

I use high-frequency prices to non-parametrically construct the continuous variation (CV), the jump variation (JV) and the jump tail index (JX). The constructed variables are then used in a HAR-VAR Kalman filter approach to provide the expected continuous variation and the expected jump tail index EJX. I also use the daily closing prices to calculate short- and medium-horizon returns for the aggregate market.

Portfolio Returns

I employ daily returns for Small and Big companies, Growth and Value companies, and High and Low momentum portfolios. The size of the firms is determined by their market equity in June of each year. The Small (Big) firms here are those in the lowest (highest) 10 percent quantiles. The Growth (Value) firms are those with book-to-market ratio in the lowest (highest) 10 percent quantiles. For momentum portfolios, the High (Low) momentum portfolio consists of past "Winners" ("Losers"), defined by the top (bottom) 10 percent of firms based on their performance in the past 2-13 months.[38]

In Table 5.1, the first four columns summarize statistics for the S&P 500 returns and the three Fama-French portfolios. On average, "Small-Big" earns an annual rate of 2.09%, "Value-Growth" earns an annual rate of 1.63%, and "Winners-Losers" portfolio earns an annual rate of 11.61% with the highest Sharpe ratio at 0.34.

Other Financial and Macro Variables

I also use the National Financial Condition Index (NFCI) from the Federal Reserve Bank of Chicago. This is a weekly index that provides information on financial conditions in US money markets, debts and equity markets. A positive (negative) NFCI signifies a tight (loose) financial condition. The default spread (DEF) refers to the difference between Moody's BAA bonds and AAA corporate bond yields. The term spread (TERM) is the difference between the 10-years bond yield and 3-month T-bill rate. The NFCI and all data needed to calculate the default spread and the term spread are downloaded from the Federal Reserve Bank of St. Louis.

In addition, I rely on five more macro-economic indicators. The Aruoba-Diebold-Scotti Business Conditions Index (ADS) from the Federal Reserve Bank of Philadelphia, which tracks real business conditions at a weekly frequency. A higher ADS generally indicates better real business conditions. Housing Starts from the U.S. Census Bureau, which tracks the total house start units. The consumer price index (CPI),

[38]These portfolios are downloaded from Professor Kenneth French's website, where detailed information is available.

industrial production (INDPRO), and the U-Michigan consumer sentiment (UMCSENT) are all obtained from the Federal Reserve Bank of St. Louis. All these financial and macro variables are converted to monthly frequency at the options' expiration date.

Table 5.1 Summary Statistics

This table reports summary statistics and correlations for monthly returns of the S&P 500, SMB (Small-Big), HML (High-Low Book-to-Market) and WML (Winners-Losers), their respective jump parts of the equity risk premium, the continuous and the jump parts of the variance risk premium, and VIX (CBOE). The data sample ranges from January 1996 to December 2011. All variables are in annualized percentages.

Panel A: Summary Statistics

	SP500	SMB	HML	WML	$ERPJ_{SP500}$	$ERPJ_{SMB}$	$ERPJ_{HML}$	$ERPJ_{WML}$	VRP^{cv}	VRP^{J}	VIX
Mean	4.76	2.09	1.63	11.61	6.75	-1.72	-1.66	-0.22	2.04	1.96	6.24
Std. Dev	19.00	17.98	19.72	34.13	1.31	0.43	0.35	0.86	0.81	0.51	1.92
Skewness	-1.36	-0.49	-0.17	-0.99	0.88	-1.31	-0.25	-2.11	5.97	0.68	4.43
Kurtosis	7.51	8.24	5.81	8.32	3.56	6.55	5.48	10.66	57.81	15.14	30.47
Max	156.58	260.76	255.60	380.16	20.95	1.67	3.05	8.49	30.89	12.09	58.02
Min	-344.30	-325.44	-255.60	-606.96	-2.08	-9.59	-6.43	-17.38	0.00	-8.71	0.93
AC1	-0.04	0.17	0.07	0.04	0.54	0.41	0.38	0.65	0.31	0.38	0.70

Panel B: Correlation Matrix

	SP500	SMB	HML	WML	$ERPJ_{SP500}$	$ERPJ_{SMB}$	$ERPJ_{HML}$	$ERPJ_{WML}$	VRP^{cv}	VRP^{J}	VIX
SP500	1.00	-0.01	0.23	-0.35	-0.10	0.15	0.12	0.06	0.25	0.14	0.04
SMB		1.00	0.36	-0.06	-0.26	0.28	0.18	0.18	-0.02	-0.03	-0.18
HML			1.00	-0.44	-0.24	0.31	0.27	0.08	0.17	0.13	-0.05
WML				1.00	0.04	-0.13	-0.19	0.09	-0.36	-0.28	-0.17
$ERPJ_{SP500}$					1.00	-0.95	-0.70	-0.56	0.29	0.44	0.51
$ERPJ_{SMB}$						1.00	0.78	0.49	-0.13	-0.15	-0.43
$ERPJ_{HML}$							1.00	-0.16	0.21	0.04	-0.04
$ERPJ_{WML}$								1.00	-0.56	-0.38	-0.69
VRP^{cv}									1.00	0.61	0.75
VRP^{J}										1.00	0.41
VIX											1.00

5.2 Estimation of Jump Intensity Measures

Shifting Jump Shape

On average, the risk-neutral left-jump shape is 14.93. This is much smaller than the right-jump shape, implying a smaller decay rate for negative jumps. The shape premium is on average 3.98, indicating a positive dynamic response between the total wealth return and the aggregate equity market.[39]

The estimated jump shapes are all time-varying. Figure 5.1 plots the inverse of the estimated jump shape parameters for the left $1/\alpha_t^{\mathbb{Q}-}$(and $1/\alpha_t^{-}$) in the top panel, and for the right $1/\alpha_t^{\mathbb{Q}+}$ (and $1/\alpha_t^{+}$) in the

[39]This number is quite similar to the calibrated risk aversion parameter $\gamma = 4$ in the rare disaster literature.

bottom panel. The stars in the top panel show that the risk-neutral left-jump distribution clearly becomes extremely fat tailed in the late 2008 financial crisis, with an unprecedented low decay rate of 1/0.249.[40] In the same panel, the $\mathbb{P}$-measure left-jump shape shows a similar dynamic pattern, but almost always with a faster decay rate than the corresponding $\mathbb{Q}$-measure variable, which comes from a positive shape premium, $\alpha_t^- = \alpha_t^{\mathbb{Q}-} + \gamma_{J,t}$. This suggests that total wealth return is almost always co-jumping with the aggregate market return in the same direction.

To better understand the source of the variation in the jump shapes, I correlate them with some selected financial indicators and macro variables in Table 5.2. The inverse of the left-jump shapes ($1/\alpha_t^{\mathbb{Q}-}$ and $1/\alpha_t^-$) are both highly correlated with NFCI and DEF. At the same time, these shape parameters are both negatively correlated with real business condition (ADS) and consumer sentiment (UMCSEMT). This suggests that when economics conditions worsen, the aggregate equity market is expected to have a higher probability for extremely large jumps. Conversely, the left-jump shape may be seen as signaling overall financial and real economic conditions—a heavier left tail indicates a worsened state of the economy for any type of investment.

The right-jump shape also changes over time. However, at each point of time, $\alpha_t^{\mathbb{Q}+} > \alpha_t^{\mathbb{Q}-}$ and $\alpha_t^+ > \alpha_t^-$, which means under both measures, the right-jump shape is always thinner, or decays faster, than the left one. Interestingly, in late 2008, the inverse of the right-jump shape parameter has an upward spike. When the equity market suffered from a significant loss in September 2008, and news spread quickly about the multiple failures of financial institutions, a strong and quick recovery was also expected to occur in the following months.[41]

Time-varying Jump Intensity

The estimated $\mathbb{Q}$-measure jump intensity has a mean of 1.00 implying one jump every year, while the $\mathbb{P}$-measure jump intensity is much smaller with a mean of 0.21 suggesting one jump every 5 years.

In parallel to the shifting jump shapes, the jump intensities under both measures are also time-varying. As shown in Figure 5.2, the $\mathbb{P}$-measure jump intensity has several peaks over the entire sample, the largest one in late 2001 caused by the 9-11 attacks. This intensity also spikes up in other periods, e.g. the 1997-1998 Asian financial crisis, the 2002 dot-com bubble, the 2008 US financial crisis and the 2010-2011 European debt

[40] This also means four moments exist for the aggregate market return process.

[41] In general, the right-jump shape is less smooth; one possible reason is the small sample problem— for each month, there are on average 85(67) calls for the entire sample from 1996-2011 (early sample 1996-2007).

crisis.

The $\mathbb{Q}$-measure intensity (stars) is persistent (first autocorrelation equals 0.42), with a subtle descending trend from year 1996 to year 2005. Table 5.2 shows this downward trend is also correlated with industrial production (-0.53) and the consumer price index (-0.49).[42] Compared with the $\mathbb{P}$-measure jump intensity, the $\mathbb{Q}$-measure intensity (the stars) is almost always larger, implying a stochastic intensity premium.[43]

Based on the shape estimates and the intensity estimates under both measures, I construct the equity risk premium for the aggregate market. Consistent with the idea of risk-return trade-off, the resulting left-jump part of the equity risk premium ($ERPJ_t^-$) is almost always positive, and the right-jump part ($ERPJ_t^+$) is almost always negative. I also obtain the volatility part of the equity risk premium ($ERPV_t$) based on a small calibration study detailed in appendix D.[44]

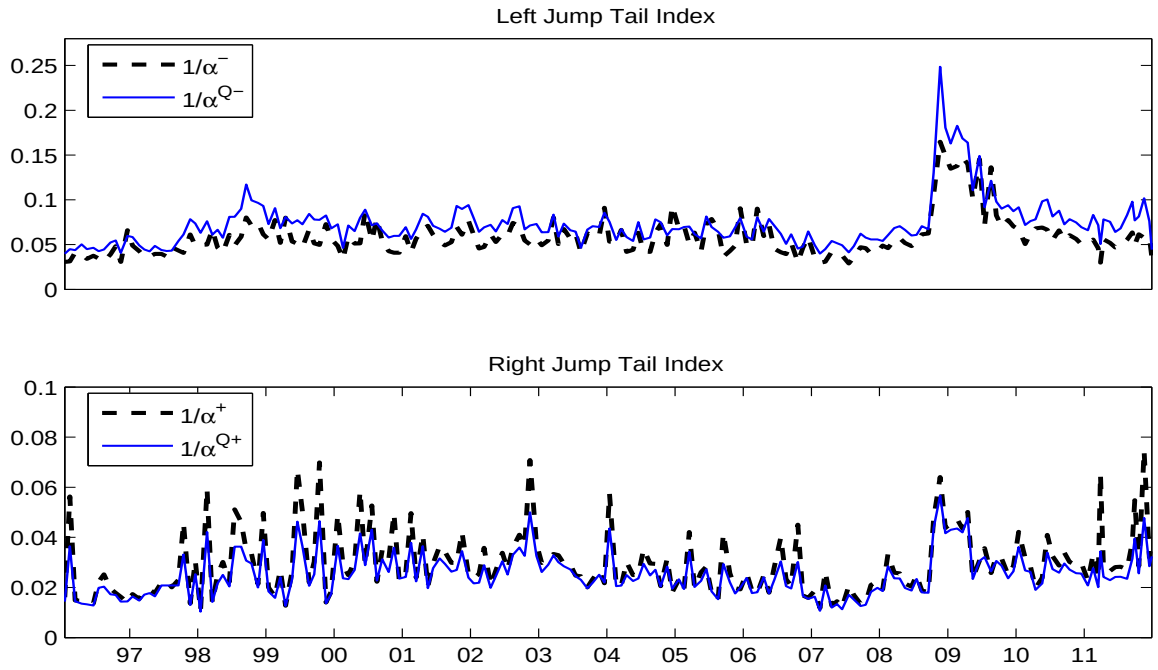

Figure 5.1 Jump Tail Index

This figure plots the inverse of the estimated left-jump (right-jump) shape parameters under the physical ($\mathbb{P}$) and risk-neutral ($\mathbb{Q}$) measures in the top panel (bottom panel). Section 4 explains the detailed estimation procedures. The sample runs from January 1996 to December 2011.

[42] The reason why the jump intensity under $\mathbb{Q}$ measure has strong negative correlation with CPI and INDPRO is not the focus of this paper, but it might be interesting for future research.

[43] To further highlight this, I also calculate the 95% confidence intervals for the estimated $\mathbb{P}$- measure jump intensity. These confidence bands are tight enough to exclude the trajectory of the $\mathbb{Q}$-measure intensity. Empirical results show that the log difference between $\mathbb{Q}$ and $\mathbb{P}$-measure intensities mostly comes from the stochastic intensity premium.

[44] Section 4 and appendix A explain the relation between $ERPV_t$ and the continuous part of the variance risk premium (VRP_t^{cv}).

Table 5.2 Jump Intensity Measures and Economic Indicators

This table reports correlations for the left-jump shapes and two jump intensities with some selected financial variables: National Financial Condition Index (NFCI), the default spread (DEF), the term spread (TERM); and with some selected macro-variables: total houses start units (HouseStart), consumer price index (CPI), industrial production (INDPRO). The sample ranges from January 1996 to December 2011.

	NFCI	DEF	TERM	ADS	HouseStart	CPI	INDPRO	UMCSENT
$\frac{1}{\alpha_t^{Q-}}$	0.75	0.75	0.28	-0.56	-0.39	0.27	-0.01	-0.40
$\frac{1}{\alpha_t^{-}}$	0.65	0.68	0.24	-0.52	-0.27	0.22	-0.01	-0.32
λ_t^Q	-0.13	-0.19	-0.07	0.20	0.04	-0.49	-0.53	0.27
λ_t	0.42	0.34	0.18	-0.20	-0.35	0.22	0.04	-0.33

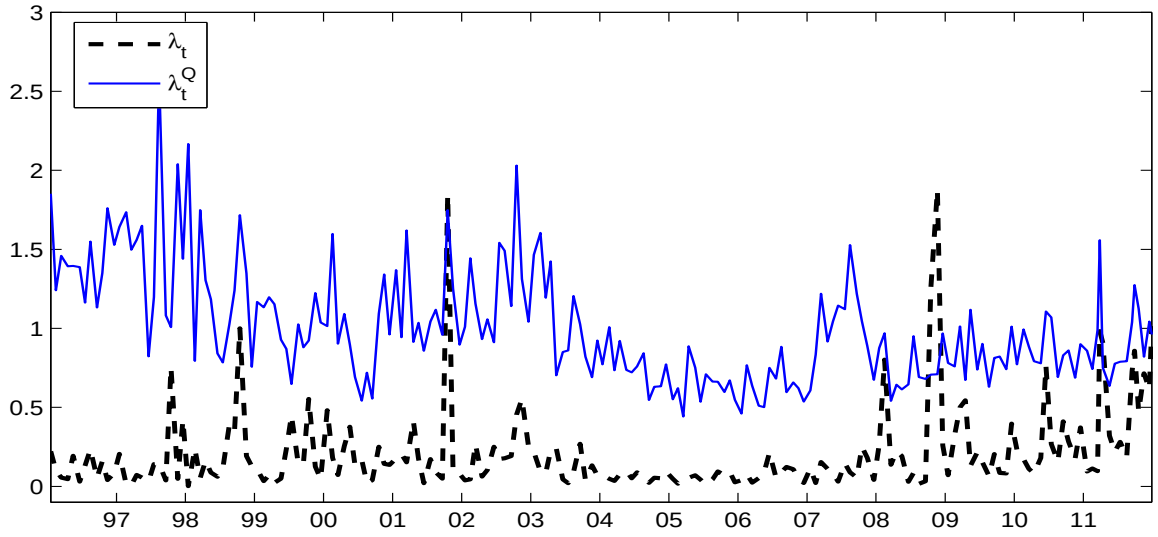

Figure 5.2 Jump Intensity

This figure plots the estimated jump intensity (physical measure as a dashed line and risk-neutral measure as a solid line). The shaded area represents the 2-standard error bands for the physical jump intensity. Section 4 explains the detailed estimation procedures. The data sample runs from January 1996 to December 2011.

5.3 Equity Risk Premium for the Aggregate Market

In Figure 5.3, I show the time-series of the jump and volatility parts of the equity risk premium ($ERPJ = ERPJ^+ + ERPJ^-$ and $ERPV$). On average, the jump part equals 6.75%, more than ten times larger than the volatility part on an annual basis. Both parts have peaks that are aligned with economic downturns and major financial events (the unconditional correlation between $ERPJ$ and $ERPV$ is 0.29), but in general they exhibit very different trajectories. Interestingly, the peaks in the jump part appear relatively stable over time. For example, the October 1997 Asian currency crisis is associated with a 19.03% premium from jumps, the August 1998 Russian bond and LTCM crises triggers a rise of $ERPJ$ to 20.94%, and these premia are not much different from the 2007-2008 US financial crisis when $ERPJ$ attains 19.98%. By contrast, before 2007 the volatility part has only moderate peaks, ranging from 0.56% to 1.63%, but then in Nov 2008, it soars up to 6.43% . There are additional peaks in both $ERPJ$ and $ERPV$ in connection with the September 11, 2001 terrorist attack, the July 2002 dot-com bubble, and the 2010-2011 European debt crisis. In all these events, the jump part of the equity risk premium captures a large increased fear for the market's decline, and the magnitude of these premia are about four times higher than the volatility part. Compared to other tail risk measures with dramatic peaks in late 2008, the magnitude of my $ERPJ$ is much smaller.[45] Since the volatility rises to unprecedented high levels in October and November 2008, the contributions from both the jump and volatility parts offset each other and become more even in comparison with other more quiet periods.

Since the jump part of the equity risk premium is constructed by the sum of the left $ERPJ_t^-$ and the right $ERPJ_t^+$ sub-parts, it is instructive to discuss the difference between this left and right decomposition for some particular event. Among all the peaks in ERPJ (=$ERPJ_t^- + ERPJ_t^+$), the left part $ERPJ_t^-$ have dominating effects over the right part $ERPJ_t^+$, and together they deliver positive risk premia. However, a reverse scenario occurs in late 2008, especially in October and November, where $ERPJ_t^-$ reaches its lowest point at -2.14% and -9.35%, and $ERPJ_t^+$ reaches its highest point at 10.46% and 29.33%. This means that the moderate positive tail risk compensation is manifest in the right jumps, not the left jumps. This counter-intuitive result is generated by the flexible dynamic response of total wealth return to the aggregate equity market $\gamma_{J,t}/\gamma$. As the total capital market value drops, the aggregate equity market is no longer a good proxy for total wealth return, inducing a sharp decrease in the shape and intensity risk premiums. Furthermore, in these two

[45] For example, the jump tail index (JTIX) in Du and Kapadia (2012) has a 50-fold increase and the jump part of the equity risk premium in Bollerslev and Todorov (2011b) reaches 40% on an annual basis.

months, financial investors were under extremely tight financial conditions: NFCI rose to unprecedented high numbers of 2.6500 and 2.7400.[46]

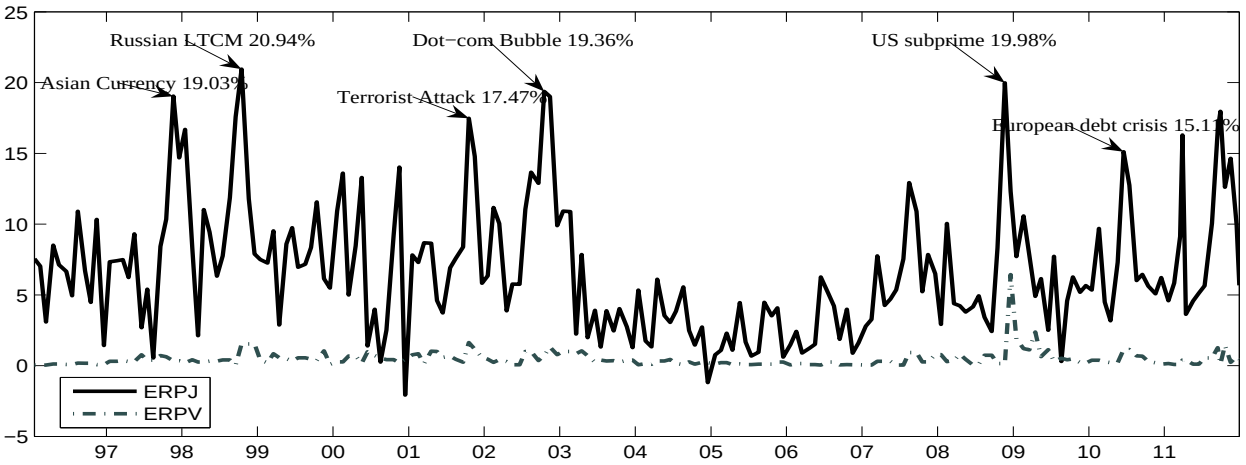

Figure 5.3 Decomposition of Equity Risk Premium

This figure plots the jump part of the equity risk premium $ERPJ_t$ as a solid line and the volatility part of the equity risk premium $ERPV_t$ as a dashed line. The data runs from January 1996 to December 2011.

5.4 Equity Risk Premia for the Fama-French Portfolios

To complement the results for the aggregate market portfolio, I also study the jump (left and right), and volatility parts of the equity risk premium for three Fama-French portfolios: SMB (small minus big firms), HML (value minus growth firms) and WML (winner minus loser firms). The constructions of these premia certainly involve the estimates of the beta loadings for each portfolio.

To start the beta pricing implications, I first split the entire data sample into three groups: the right-jump period, the left-jump period and the calm period, each of which is defined as the collection of days when the S&P500 intra-day price jumps were larger than 0.6%, smaller than −0.6%, or no such jumps, respectively.[47] The rationale for this split is to select days when the market is likely to experience large rare jumps and use those selected days to separately estimate the beta coefficients for the right-jump, left-jump and volatility.

[46]National financial condition index (NFCI) summarizes the overall conditions of money markets, debt and equity markets, and these extremely large positive values of the NFCI indicate all three markets are risker, with low liquidity and high leverage.

[47]The cutoff choice 0.6% is adopted from Bollerslev and Todorov (2011b). It is large enough to select large jumps and small enough to identify a reasonable number of jumps in the sample.

Formally, for each portfolio i, I run three regressions,

$$r_{i,t}DM_t^{J^+} = \beta_{i,0}^{J^+}\ r_{m,t}DM_t^{J^+} + e_{t,J^+}, \tag{5.1}$$

$$r_{i,t}DM_t^{J^-} = \left(\beta_{i,0}^{J^-} + \frac{\beta_{i,1}^{J^-}}{\alpha_t^{\mathbb{Q}-}}\right)\ r_{m,t}DM_t^{J^-} + e_{t,J^-}, \tag{5.2}$$

$$r_{i,t}DM_t^{\sigma} = \left(\beta_{i,0}^{\sigma} + \frac{\beta_{i,1}^{\sigma}}{\alpha_t^{\mathbb{Q}-}}\right)\ r_{m,t}DM_t^{\sigma} + e_{t,\sigma}. \tag{5.3}$$

where $r_{i,t}$ and $r_{m,t}$ are daily log returns, $DM_{\cdot}$ are dummy variables to indicate the three different scenarios, $\beta_{i,0}^{\sigma}, \beta_{i,1}^{\sigma}, \beta_{i,0}^{J^+}, \beta_{i,0}^{J^-}$ and $\beta_{i,1}^{J^-}$ are the betas for the continuous shocks, the right jumps and the left jumps in equation (2.4).

Table 5.3 reports the beta estimates for the SMB, HML and WML portfolios. For each portfolio, I have 101 days to estimate $\beta_{i,0}^{J^+}$, 99 days for $\beta_{i,0}^{J^-}$ and $\beta_{i,1}^{J^-}$, and 3746 "normal" days for $\beta_{i,0}^{\sigma}$ and $\beta_{i,1}^{\sigma}$. In line with the literature, on average, I find that SMB, HML and WML portfolios all tend to load negatively on both the left and negative market jumps. What is more interesting here is the time-varying beta estimates in the fifth row in Table 5.3. In contrast to the right-jump beta, the left-jump beta and the volatility beta both significantly change with the jump shape parameter $\frac{1}{\alpha_t^{\mathbb{Q}-}}$. This means when financial conditions become tighter and the aggregate market has a negative jump, the Small-Big and the Value-Growth portfolio jumps in the same direction, but the Winners-Losers portfolio jumps in the opposite direction. These differences in the beta estimates naturally result in more variation in the equity risk premiums for the different portfolios.

Together with the market jump intensity and the jump shape estimates, I first investigate the resulting jump parts, then the volatility parts of the portfolios' equity risk premia. Figure 5.4 plots the right (dashed line) and left (solid line) jump parts of the equity risk premium for each portfolio in separate panels. In most months, the negative beta loadings for the right market jump for all three portfolios imply positive risk premiums. Comparing across the different portfolios, all three right-jump parts ($ERPJ_{i,t}^{+}$) are highly correlated with each other, since the variation mainly comes from the counterpart to the market $ERPJ_t^{+}$. Conversely, the three left-jump parts ($ERPJ_{i,t}^{-}$) are very different dynamically. This may be explained by the different stochastic betas for the negative market jumps. Specifically, in October and November of 2008, this premium almost disappears for the SMB portfolio. For HML it starts from around zero and then drops down to be negative. For WML it also starts from around zero but rises back to 10.44%. These differences come from the dual impacts of the different beta loadings and the unique market conditions. For example,

	SMB			HML			WML		
	J^+	J^-	V	J^+	J^-	V	J^+	J^-	V
Constant	-0.009	0.004	0.032	-0.003	-0.001	0.017	0.009	0.000	0.040
std	(0.003)	(0.002)	(0.015)	(0.004)	(0.002)	(0.016)	(0.008)	(0.004)	(0.029)
β_0	-0.434	-0.338	-0.512	-0.135	-0.417	-0.375	-0.818	0.288	0.379
std	(0.079)	(0.099)	(0.055)	(0.098)	(0.157)	(0.083)	(0.163)	(0.234)	(0.177)
β_1		1.169	1.831		2.951	3.837		-5.849	-7.386
std		(0.694)	(0.530)		(0.987)	(0.869)		(1.669)	(2.150)
$R2$	40.494	21.766	25.256	3.196	10.097	4.467	24.723	26.412	9.271

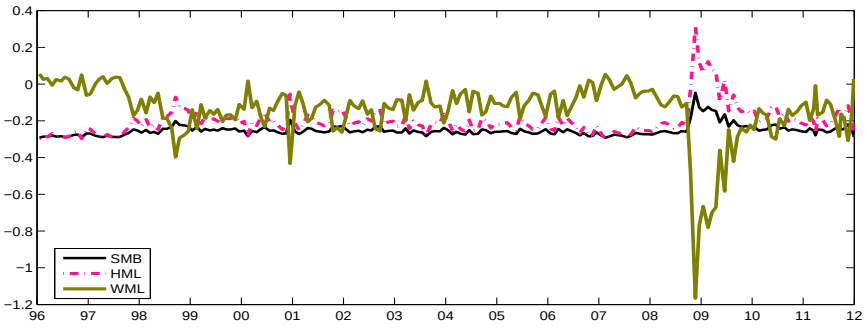

Table 5.3 Beta Loadings

The top panel reports the beta estimates for SMB (left panel), HML (middle panel) and WML (right panel) portfolios, for each portfolio, I estimate right-jump beta (J^+), left-jump beta (J^-) and calm period beta (V). For each type, $\beta_t = \beta_0 + \beta_1/\alpha_t^{\mathbb{Q}-}$ in equation (5.1). The bottom panel is the time-series plot for the left-jump betas, $\beta_{i,t}^{J^-} = \beta_{i,0}^{J^-} + \beta_{i,1}^{J^-}/\alpha_t^{\mathbb{Q}-}$. Daily portfolio returns come from professor Kenneth French's website and high-frequency data for the S&P 500 futures come from TAQ dataset. The sample runs from 01Jan1996 to 31Dec2011.

in November 2008, the left-jump beta for HML is -0.0477, compared to the left-jump beta for WML equal to -1.1660, but it also has a lower associated premium implied by the negative market-wide intensity premium.

Lastly, Figure 5.5 shows the total jump and the volatility parts of the equity risk premiums for the three portfolios. The volatility parts are almost always smaller in magnitude. Interestingly, the jump parts of the portfolios' equity risk premia exhibit very different dynamic patterns. The SMB jump premium is strongly negatively correlated with market's counterpart (correlation equals -0.95), and positively related with that of HML (0.78) and WML (0.49). The HML and WML jump premia, on the other hand, correlate negatively with the market's counterpart at -0.70 and -0.56. Unlike most of the beta pricing studies, the portfolios' equity risk premia here are not linearly related to that of the market. These additional sources of variations come from the fact that: [1] the jump shapes shift through time, and the beta loadings enter into the premium in a nonlinear fashion; [2] the beta loadings for the left-jumps also change with different financial conditions.

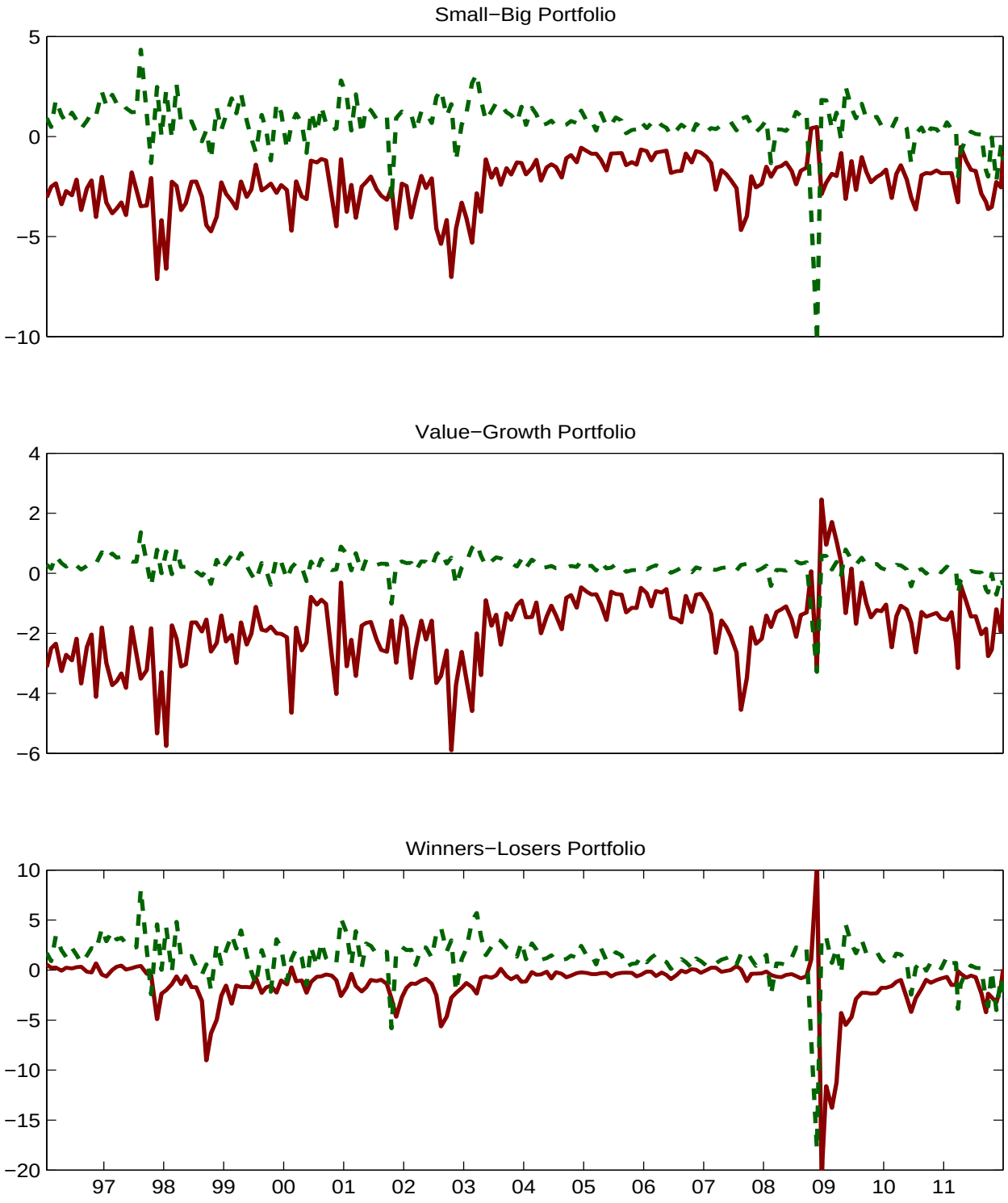

Figure 5.4 Decomposition of Jump parts of Portfolios' Equity Risk Premium

This figure plots right and left jump risk premiums for SMB, HML and WML. The constructions are based on tail shape parameters $\frac{1}{\alpha_t^{\mathbb{Q}\pm}}$ and $\frac{1}{\alpha_t^{\pm}}$, the intensities $\lambda_t^{\mathbb{Q}}$ and λ_t, and the beta estimates in Table 5.3. The sample runs from January 1996 to December 2011.

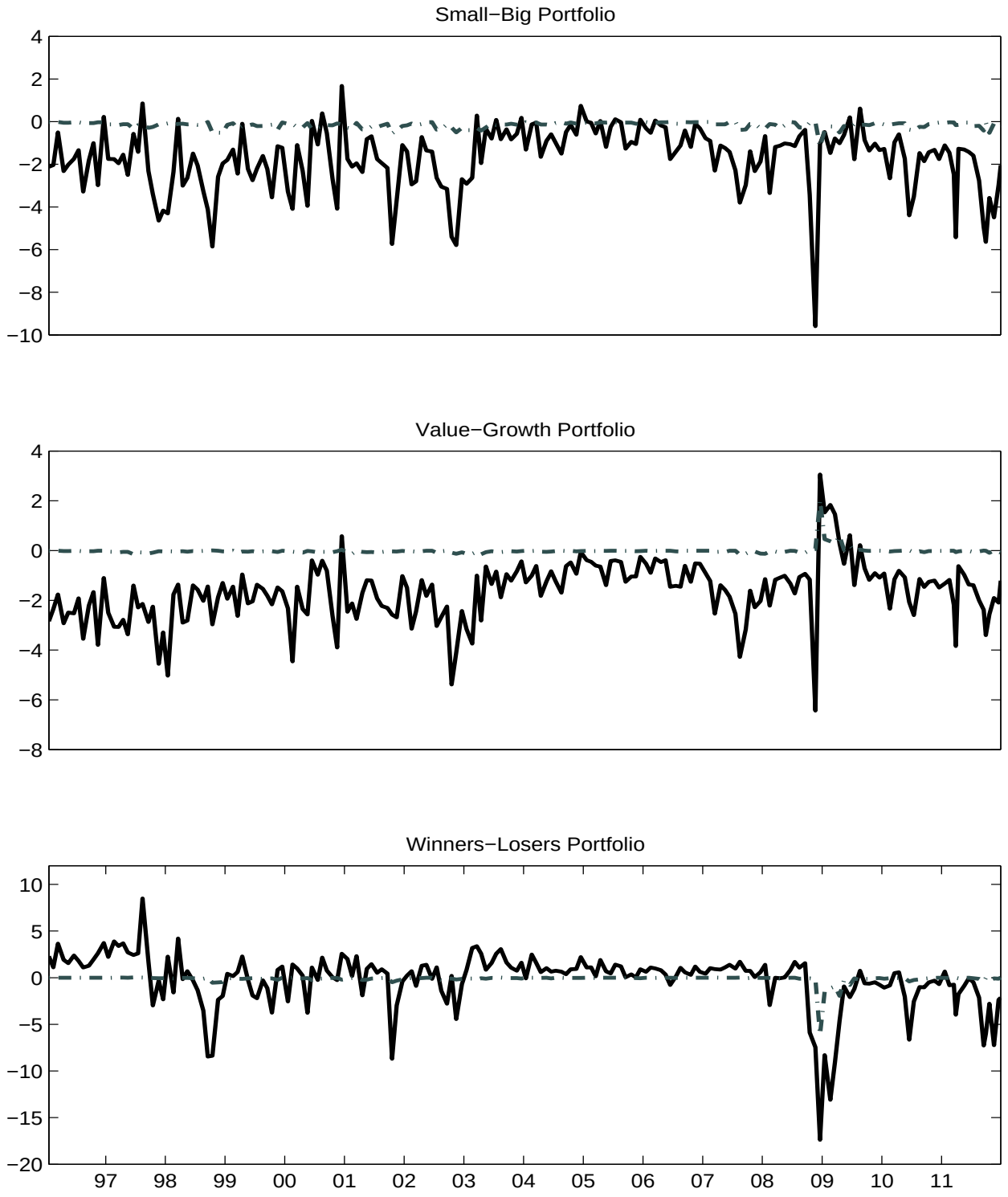

Figure 5.5 Decomposition of Portfolios' Equity Risk Premium

This figure plots the jump and diffusive risk premiums for SMB, HML and WML. The construction are based on tail shape parameters $\frac{1}{\alpha_t^{\mathbb{Q}\pm}}$ and $\frac{1}{\alpha_t^{\pm}}$, the intensities $\lambda_t^{\mathbb{Q}}$ and λ_t, and the beta estimates in Table 5.3. The sample runs from January 1996 to December 2011.

5.5 Return Predictability Studies

I now turn to the study of the long-term equity risk premium. In my model, the long-term equity risk premium (from time t to $t + n\tau$) is the summation of the expected instantaneous equity risk premium, defined as $ERP_{t,n\tau} \equiv \sum_{j=1}^{n} E_t ERP_{t+j\tau}$. If $ERP_{t,n\tau}$ can be approximated by some observables X_t, then we should have the empirical regressions,

$$\sum_{j=1}^{n} r_{t+(j-1)\tau,t+j\tau} = a(n) + b^{'}(n)X_t + \epsilon_{r,t+j\tau}. \tag{5.4}$$

where $\sum_{j=1}^{n} r_{t+(j-1)\tau,t+j\tau}$ is the compounded asset return, a noisy but unbiased proxy for the long-term risk premium. If X_t can strongly predict the future compounded asset return, then X_t is a good approximation for the long-term equity risk premium.

Table 5.4 presents these predictability studies at a one-month horizon. I try three measures of $\widehat{ERP}_t$: my proposed measure with shifting jump shapes and self-exciting intensity (top panel), a benchmark measure with constant jump shapes (middle panel) and another benchmark measure with constant jump shapes and without self-exciting jump intensity (bottom panel). For each measure, I choose three sets of X_t in the empirical regressions: [1] the jump and the volatility parts of the equity risk premium ($ERPJ$ and $ERPV$); [2] the deeper tails of the jump part of the equity risk premium ($ERPJ(VIX)$);[48] [3] the jump part of the variance risk premium (VRP^J).

Across different columns in Table 5.4, my proposed measure for X_t has uniformly superior predictive power for the one-month S&P 500 return. For example, $ERPJ$ has R^2 equal to 1.33%, compared to 1.00% for $ERPJ^*$ and 0.96% for $ERPJ^{**}$. By adding in the volatility part in a joint regression, my proposed measure maintains the strongest predictive power of a total R^2 equal to 2.79% and adjusted R^2 equal to 1.77%. If one uses a deeper tail ($ERPJ(VIX)$) together with $ERPV$, the resulting R^2 equals 2.43%, which is 1.00% higher than the first corresponding benchmark variable ($ERPJ^*(VIX)$ and $ERPV^*$) and 1.83% higher than the second benchmark variable ($ERPJ^{**}(VIX)$ and $ERPV^{**}$). Moreover, the variance risk premium $X_t = [VRP^{cv},\ VRP^J]$ of all measures have relatively weaker return forecastability. The time-variation of the jump shapes and the self-excitation of the jump intensity are both essential to the one-month equity risk premium for the aggregate market.

[48] The deeper tail $ERPJ(VIX)$ refers to a subset $\mathbb{D}$ in equation (4.9), where $\mathbb{D} = [-\infty, k_t^{**-}] \bigcup [k_t^{**+}, \infty]$, $k_t^{**-} = -2.0 \times VIX_t \sqrt{\tau}$, $k_t^{**+} = 1.75 \times VIX_t \sqrt{\tau}$, and τ= 30 calender days.

This comparison also holds as the compounded horizon increases. In Figure 5.6, from one to six months, the proposed $X_t = [ERPJ \;\; ERPV]$ has uniformly stronger predictive power compared to the benchmark $X_t = [ERPJ^{**} \;\; ERPV^{**}]$. The R^2 for returns has a hump shape pattern peaking at a three-month horizon, consistent with the hump first documented by Bollerslev et al. (2009) and later by Bollerslev et al. (2011). However, in the sample period considered in this paper, the forecasting power of the total VRP_t stays below 1% throughout the short-median horizon. This suggests that the tail risk is indeed very different from the diffusive risk.

Table 5.5 presents prediction results for the three portfolios Small-Big (SMB Top Panel), Value-Growth (HML Middle Panel) and Winners-Losers (WML Bottom Panel). The first four columns show that the deeper tails of the jump components explain larger amount of the portfolios' one-month equity risk premiums. The volatility parts help to increase SMB return predictability, but not significantly for HML and WML returns. In particular, the SMB portfolio can be explained by $X_t = [ERPJ_{SMB}(VIX) \;\; ERPV_{SMB}]$ with $R^2 = 7.07\%$, and the WML portfolio can be explained by $X_t = [ERPJ_{WML}(VIX) \;\; ERPV_{WML}]$ with $R^2 = 4.54\%$. The last two columns show the variance risk premium has limited contribution to the portfolios' return predictability. These results suggest that the portfolios' beta loadings are time-varying and their long-term equity risk premiums are better captured by their own instantaneous equity risk premium rather than the variance risk premium of the aggregate market.

Figure 5.7 plots the R^2s in the portfolio return predictions. For all three portfolios, the predictive power of the deeper tails are stronger than the total jump components. The R^2s are almost all increasing from one to six month horizons and no hump shape is detected at the shorter horizons.

Table 5.4 One-Month S&P 500 Return Prediction

This table reports the compounded return predictions based on three measures (with various components) of the equity risk premium. The return process is S&P 500; ERP represents the proposed measure with the shifting jump shapes and the self-exciting jump intensity; ERP* restricts the shape to be constant, and ERP** further restricts the jump intensity to be not self-exciting. The constants and their associated standard errors are scaled by 100. The data sample ranges from January 1996 to December 2011. All measures of the equity risk premiums are in monthly units.

	S&P 500 Returns					
Constant	-0.57	-0.80	-0.37	-0.59	0.19	0.23
std	(0.77)	(0.73)	(0.74)	(0.71)	(0.54)	(0.50)
ERPJ	1.67		2.19			
std	(0.83)		(0.92)			
ERPJ(VIX)		2.86		3.41		
std		(1.28)		(1.31)		
ERPV			-2.92	-2.54		-3.68
std			(1.12)	(1.09)		(1.56)
VRP^J					1.08	4.65
std					(2.96)	(3.35)
R^2	1.33	1.29	2.79	2.43	0.08	1.67
Adjusted R^2	0.82	0.78	1.77	1.41	-0.44	0.64
Constant	0.01	-0.17	0.56	0.22	0.12	0.67
std	(0.42)	(0.53)	(0.53)	(0.58)	(0.42)	(0.53)
ERPJ*	0.46		0.66			
std	(0.23)		(0.26)			
ERPJ(VIX)*		1.21		1.51		
std		(1.25)		(1.35)		
ERPV*			-4.91	-3.75		-4.44
std			(3.55)	(3.35)		(3.55)
VRP^{J*}					0.95	1.29
std					(0.43)	(0.47)
R^2	1.00	0.63	2.28	1.44	0.87	1.95
Adjusted R^2	0.49	0.11	1.26	0.41	0.35	0.92
Constant	0.05	0.25	0.61	0.61	-0.11	0.39
std	(0.42)	(0.56)	(0.53)	(0.61)	(0.45)	(0.53)
ERPJ**	0.43		0.60			
std	(0.20)		(0.23)			
ERPJ(VIX)**		0.31		0.54		
std		(1.76)		(1.89)		
ERPV**			-4.84	-3.10		-5.02
std			(3.56)	(3.30)		(3.55)
VRP^{J**}					7.70	11.04
std					(4.28)	(4.85)
R^2	0.96	0.03	2.21	0.60	1.05	2.37
Adjusted R^2	0.45	-0.49	1.18	-0.45	0.53	1.35

Table 5.5 One-Month Portfolio Returns Prediction

This table reports the compounded returns predictions based on three measures (with various components) of the equity risk premium. The return processes are the SMB, HML and WML portfolios. ERP represents the proposed measure with the shifting jump shapes and the self-exciting jump intensity. The constants and their associated standard errors are scaled by 100. The data samples range from January 1996 to December 2011. All measures of the equity risk premium are in monthly units.

	SMB Returns					
Constant	1.14	2.36	0.67	1.91	0.18	-0.05
std	(0.50)	(0.72)	(0.51)	(0.62)	(0.48)	(0.50)
$ERPJ_{SMB}$	6.75		7.83			
std	(2.41)		(2.94)			
$ERPJ_{SMB}$(VIX)		19.11		20.46		
std		(5.74)		(6.17)		
$ERPV_{SMB}$			-10.61	-10.29		-10.41
std			(6.75)	(6.17)		(8.57)
VRP^J					-0.04	-2.40
std					(2.14)	(3.39)
R2	2.65	5.70	4.06	7.07	0.00	0.98
Adjusted R^2	2.14	5.21	3.06	6.10	-0.52	-0.06

	HML Returns					
Constant	0.30	1.51	0.49	2.01	0.88	0.94
std	(1.11)	(0.84)	(1.19)	(0.90)	(0.55)	(0.59)
$ERPJ_{HML}$	1.20		2.77			
std	(6.85)		(7.68)			
$ERPJ_{HML}$(VIX)		14.86		20.65		
std		(7.28)		(8.45)		
$ERPV_{HML}$			-5.11	-10.69		1.56
std			(5.36)	(3.64)		(3.79)
VRP^J					-4.61	-4.92
std					(2.93)	(3.32)
R^2	0.04	2.04	0.33	3.31	1.42	1.45
Adjusted R^2	-0.48	1.53	-0.71	2.30	0.90	0.41

	WML Returns					
Constant	1.09	1.80	1.29	1.80	1.91	1.33
std	(0.67)	(0.60)	(0.70)	(0.59)	(1.10)	(1.17)
$ERPJ_{WML}$	7.11		4.87			
std	(4.92)		(5.91)			
$ERPJ_{WML}$(VIX)		13.17		10.70		
std		(8.27)		(10.72)		
$ERPV_{WML}$			4.69	3.18		8.62
std			(5.59)	(5.42)		(3.31)
VRP^J					-5.76	0.45
std					(7.24)	(7.66)
R^2	3.19	4.29	3.74	4.54	0.74	2.80
Adjusted R^2	2.69	3.79	2.73	3.54	0.22	1.78

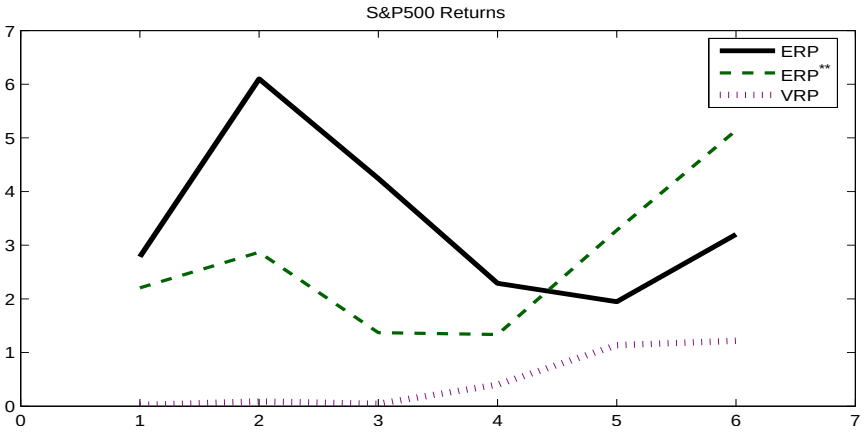

Figure 5.6 Long-Horizon Return Prediction

This figure plots the R^2% in return prediction studies from one to six months. The solid line represents the deeper tail of the jump risk premium $ERPJ(VIX)$ and the diffusive risk premium $ERPV$, the dashed line refers to the benchmark which restricts the shape to be constant with a non self-exciting jump intensity, $X_t = [ERPJ^{**}(VIX),\ \ ERPV^{**}]$. The sample ranges from January 1996 to December 2011.

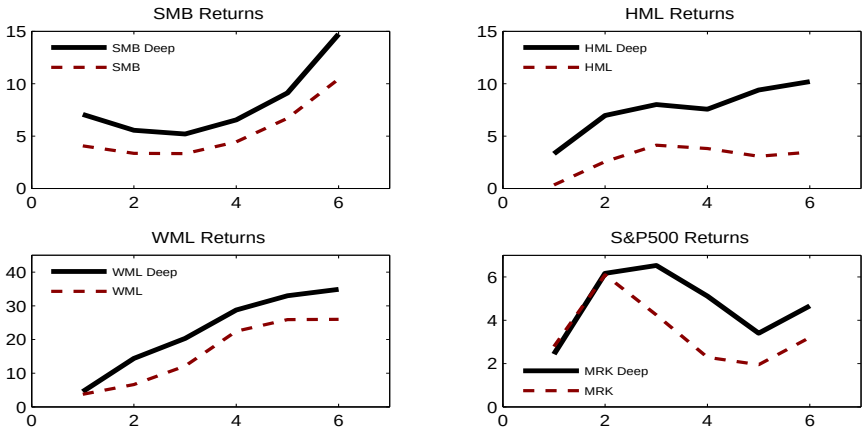

Figure 5.7 Long-Horizon Return Prediction

This figure plots the R^2% for portfolio return prediction studies from one to six months in the top panel. The solid line represents the deeper tail of the portfolio's jump risk premium $ERPJ(VIX)$ and diffusive risk premium $ERPV$, the dashed line refers to the portfolio's total jump risk premium $ERPJ$ and diffusive risk premium $ERPV$. The sample ranges from January 1996 to December 2011.

6 Conclusion

This paper provides a new approach for modeling and estimating the jump risk premium in the equity market. I show that investors dislike two types of jump risk: the frequency of the discontinuous movement and the probability that this movement is extremely large. By incorporating these two different channels, and further allowing the jump arrival rate to be self-exciting, the complex structure of the jump risk premium is no longer affine in the jump arrival rate.

The corresponding semi-parametric estimation approach developed here relies on a large panel of options and high-frequency intra-day prices to uncover the associated risk compensation. Together with the diffusive risk premium, the proposed jump risk premium is capable of providing a better description for the longer-term equity risk premium. It also helps explain differences in the returns across the three Fama-French portfolios.

A Model Solution

In this section, I explain in detail how to derive the closed-form solutions for the pricing kernel and the equity risk premia. The overall solution method is typical as in Bansal and Yaron (2004) and Drechsler and Yaron (2011), among others. The solutions derived here are crucial to understanding the risk factors and the way in which they are priced.

A.1 Equity Risk Premium

I start by conjecturing the hedging demand as a linear function of the jump intensity, the volatility factor and the risk free rate,

$$h_t = A_0 + A_q q_t + A_{\lambda,t}\lambda_t + A_f r_{f,t}. \tag{A.1}$$

where the risk free rate follows a CIR model $dr_{f,t} = \kappa_f(\mu_f - r_{f,t})dt + \varphi_f\sqrt{r_{f,t}}dW_{f,t}$, $W_{f,t}$ is an independent Brownian motion of $W_{i,t}, W_{c^\perp,t}$, $W_{m^\perp,t}$ and $W_{q,t}$, and the loading on the intensity is time-varying $\lambda_t dA_{\lambda,t} = \mu_{A_\lambda,t}\lambda_t + \varphi_{A_\lambda}dW_{A_{\lambda,t},t}$. In turn, the stochastic discount factor M_t follows a jump diffusion model as well,

$$\begin{aligned} dlnM_t &= -r_{f,t}dt - m_t dt + \sigma_t dW_t + \int_{\mathbb{B}}(-\gamma_{J,t}x + \phi_{\lambda,t})J(dt,dx), \\ \sigma_t dW_t &= -\gamma\sigma_c dW_{c^\perp,t} + \sqrt{q_t}\left(\gamma\varphi_c + \phi_q\right)dW_{q,t} + \phi_f\sqrt{r_{f,t}}dW_{f,t} + \phi_{A_\lambda}dW_{A_{\lambda,t},t}, \\ m_t &= 0.5\left(\phi_{A_\lambda}^2 + \gamma^2\sigma_c^2 + (\gamma\varphi_c + \phi_q)^2 q_t + \phi_f^2 r_{f,t}\right) + \lambda_t\int_{\mathbb{B}}(e^{-\gamma_{J,t}x+\phi_{\lambda,t}} - 1)f_t(x)dx. \end{aligned} \tag{A.2}$$

where $\phi_q = \frac{\theta}{\Psi}A_q\varphi_q$, $\phi_{\lambda,t} = \frac{\theta}{\Psi}A_{\lambda,t}\varphi_\lambda$, $\phi_f = \frac{\theta}{\Psi}A_f\varphi_f$ and $\phi_{A_\lambda} = \frac{\theta}{\Psi}\varphi_{A_\lambda}$ are pricing coefficients. The drift term m_t ensures the no arbitrage condition holds for bond pricing, and W_t summarizes the Brownian motions from hedging demand h_t and the total wealth return $R_{c,t}$. Taken together, based on a no-arbitrage condition $d(R_{c,t}M_t)$=0, the solution for the drift term $a_{c,t}$ has the following form,

$$a_{c,t} = r_{f,t} + \gamma\sigma_c^2 + \varphi_c(\gamma\varphi_c + \phi_q)q_t + \lambda_t\left(\int_B(e^{\frac{\gamma_{J,t}}{\gamma}x} - 1)f_t(x)dx - \int_B(e^{\frac{\gamma_{J,t}}{\gamma}x} - 1)e^{-\gamma_{J,t}x+\phi_{\lambda,t}}f_t(x)dx\right). \tag{A.3}$$

Lastly, to solve the pricing coefficients, I use equations (A.1)-(A.3) to substitute out corresponding terms in the Euler equation (3.2), which must hold regardless of the realization of the state vector $[q_t, r_{f,t}, \lambda_t]$.

Therefore, it follows that,

$$
\begin{aligned}
0 &= (\kappa_q + \frac{1-k_1}{k_1})A_q + (\Psi/\theta)\left(-0.5\phi_q^2 + \left(\gamma\varphi_c^2(\gamma - 0.5) - 0.5\gamma^2\varphi_c^2\right)\right), \\
0 &= (\kappa_\lambda + \frac{1-k_1}{k_1})A_{\lambda,t} + (\Psi/\theta)\left(\gamma\int_{\mathbb{R}}(1 - e^{\frac{\gamma_{J,t}}{\gamma}x})e^{-\gamma_{J,t}x+\phi_{\lambda,t}}f^{\mathbb{P}}(x)dx - \int_{\mathbb{R}}(1 - e^{\gamma_{J,t}x-\phi_{\lambda,t}})e^{-\gamma_{J,t}x+\phi_{\lambda,t}}f^{\mathbb{P}}(x)dx\right), \\
0 &= (\kappa_f + \frac{1-k_1}{k_1})A_f + (\Psi/\theta)\left(\gamma - 0.5\phi_f^2 - 1\right).
\end{aligned}
$$

Or equivalently, the pricing coefficients $\phi_\cdot$ have the following expressions,

$$
\begin{aligned}
\phi_q &= (\kappa_q + \frac{1-k_1}{k_1})/\varphi_q - \left((\kappa_q + \frac{1-k_1}{k_1})^2/\varphi_q^2 + \gamma\varphi_c^2(\gamma - 1)\right)^{1/2}, \\
\phi_{\lambda,t} &= \left(\mu_{A_\lambda,t} - \left(\gamma\int_{\mathbb{B}}(1 - e^{\frac{\gamma_{J,t}}{\gamma}x})e^{-\gamma_{J,t}x+\phi_{\lambda,t}}f_t(x)dx - \int_{\mathbb{B}}(1 - e^{\gamma_{J,t}x-\phi_{\lambda,t}})e^{-\gamma_{J,t}x+\phi_{\lambda,t}}f_t(x)dx\right)\right)\varphi_\lambda/(\kappa_\lambda + \frac{1-k_1}{k_1}), \\
\phi_f &= (\kappa_f + \frac{1-k_1}{k_1})/\varphi_f - \left((\kappa_f + \frac{1-k_1}{k_1})^2/\varphi_f^2 + 2(\gamma - 1)\right)^{1/2}.
\end{aligned}
$$

There are several things worth noticing: first, the sign of all pricing coefficients are related to the magnitude of risk aversion γ, but not the elasticity parameter Ψ. Second, if $\gamma > 1$, then $\phi_f < 0$, which means the risk free rate serves as a good hedging portfolio and is negatively priced. Third, despite $\gamma > 1$ leading to a negative ϕ_q, volatility is always positively priced as $\gamma\varphi_c + \phi_q > 0$. Lastly , the intensity premium $\phi_{\lambda,t}$ is time varying, due to its stochastic long-run mean $\mu_{A_\lambda,t}$ and the shifting jump shape.

A.2 Variance Risk Premia

Variance risk premium $VRP_{t,T}$ is the difference between the risk neutral and the physical expectations of the quadratic variance, and is also naturally decomposed into two parts $VRP_{t,T} = VRP^{cv}_{t,T} + VRP^{J}_{t,T}$,

$$
\begin{aligned}
VRP^{J}_{t,T} &\equiv -E_t\int_t^T \lambda_s\int_B x^2 f_s(x)dxds + E_t^{\mathbb{Q}}\int_t^T \lambda_s^{\mathbb{Q}}\int_B x^2 f_s^{\mathbb{Q}}(x)dxds, && \text{(A.4)} \\
VRP^{cv}_{t,T} &\equiv -E_t\int_t^T \left(\sigma_m^2 + \varphi_m^2 q_s\right)ds + E_t^{\mathbb{Q}}\int_t^T \left(\sigma_m^2 + \varphi_m^2 q_s\right)ds, && \text{(A.5)} \\
&= -E_t\int_t^T \varphi_m^2 q_s ds + E_t^{\mathbb{Q}}\int_t^T \varphi_m^2 q_s ds. && \text{(A.6)}
\end{aligned}
$$

Next, to go one step further, the conditional mean of the square root process q_t has the following expression,

$$
E_t q_{t+s} = e^{-\kappa_q s}(q_t - \mu_q) + \mu_q. \tag{A.7}
$$

and the difference between $\mathbb{Q}$ and $\mathbb{P}$ expectation is,

$$
E_t^{\mathbb{Q}} q_{t+s} - E_t q_{t+s} = q_t(e^{-\kappa_q^{\mathbb{Q}} s} - e^{-\kappa_q s}) + e^{-\kappa_q^{\mathbb{Q}} s}\mu_q^{\mathbb{Q}} - e^{-\kappa_q s}\mu_q + \mu_q^{\mathbb{Q}} - \mu_q. \tag{A.8}
$$

where $\kappa_q^{\mathbb{Q}} = \kappa_q - \varphi_q(\gamma\varphi_c + \phi_q)$, $\kappa_q^{\mathbb{Q}}\mu_q^{\mathbb{Q}} = \kappa_q\mu_q$. As such, both the expected future return variance E_tCV and the continuous part of the variance risk premium VRP_t^{cv} are affine in latent factor q_t,

$$E_t^{\mathbb{P}}CV \equiv E_t^{\mathbb{P}}\int_t^T \sigma_c^2 + \sigma_m^2 + \varphi_m^2 q_s ds = a_{4,0} + a_{4,3}q_t, \tag{A.9}$$

$$VRP_t^{cv} = a_{3,0} + a_{3,3}q_t. \tag{A.10}$$

where $ey(k) = \frac{e^{-k(T-t)}-1}{-k}$ and,

$$a_{4,0} = \sigma_c^2(T-t) + \sigma_m^2(T-t) + \varphi_m^2(T-t-ey(\kappa_q)), \quad a_{4,3} = ey(\kappa_q),$$

$$a_{3,0} = \varphi_m^2[(T-t)(\mu_q^{\mathbb{Q}} - \mu_q) - ey(\kappa_q^{\mathbb{Q}})\mu_q^{\mathbb{Q}} + ey(\kappa_q)\mu_q], \quad a_{3,3} = \varphi_m^2[ey(\kappa_q^{\mathbb{Q}}) - ey(\kappa_q)].$$

Lastly, I turn to the jump part of the variance risk premium $VRP_{t,T}^J$. By assuming the intensity premium and the shape parameters are unchanged within a short period of time $T-t$, the expectations of the self-exciting jump intensity are,

$$E_t\lambda_{t+s} = e^{-\tilde{\kappa}_\lambda s}(\lambda_t - \tilde{\mu}_\lambda) + \tilde{\mu}_\lambda, \tag{A.11}$$

$$E_t^{\mathbb{Q}}\lambda_{t+s} = e^{-\tilde{\kappa}_\lambda^{\mathbb{Q}} s}(\lambda_t - \tilde{\mu}_\lambda^{\mathbb{Q}}) + \tilde{\mu}_\lambda^{\mathbb{Q}}. \tag{A.12}$$

where $\tilde{\kappa}_\lambda = \kappa_\lambda - \varphi_\lambda$, $\tilde{\kappa}_\lambda\tilde{\mu}_\lambda = \kappa_\lambda\mu_\lambda$ and $\tilde{\kappa}_\lambda^{\mathbb{Q}} = \kappa_\lambda - \varphi_\lambda e^{\phi_{\lambda,t}}\int_B e^{-\gamma_{J,t}x} f_t(x)dx$, $\tilde{\kappa}_\lambda^{\mathbb{Q}}\tilde{\mu}_\lambda^{\mathbb{Q}} = \kappa_\lambda\mu_\lambda$. By integrating over this time period,

$$E_t\int_t^T \lambda_s ds = a_{1,0} + a_{1,1}\lambda_t, \tag{A.13}$$

$$E_t^{\mathbb{Q}}\int_t^T \lambda_s^{\mathbb{Q}} ds = e^{\phi_{\lambda,t}}\int_B e^{-\gamma_{J,t}x} f_t(x)dx \times E_t^{\mathbb{Q}}\int_t^T \lambda_s ds = a_{2,0}e^{\phi_{\lambda,t}}\int_B e^{-\gamma_{J,t}x} f_t(x)dx + a_{2,2}\lambda_t^{\mathbb{Q}}. \tag{A.14}$$

where $a_{1,0} = T-t-ey(\tilde{\kappa}_\lambda)$, $a_{1,1} = ey(\tilde{\kappa}_\lambda)$ and $a_{2,0} = T-t-ey(\tilde{\kappa}_\lambda^{\mathbb{Q}})$, $a_{2,2} = ey(\tilde{\kappa}_\lambda^{\mathbb{Q}})$. The $\mathbb{P}$- measure expectation in equation (A.4) becomes $E_t\int_t^T \lambda_s ds \times \int_{\mathbb{B}} x^2 f_t(x)dx = (a_{1,0} + a_{1,1}\lambda_t) \times \int_{\mathbb{B}} x^2 f_t(x)dx$, and the $\mathbb{Q}$- measure expectation becomes $E_t^{\mathbb{Q}}\int_t^T \lambda_s^{\mathbb{Q}} ds \times \int_{\mathbb{B}} x^2 f_t^{\mathbb{Q}}(x)dx = (a_{2,0}e^{\phi_{\lambda,t}}\int_{\mathbb{B}} e^{-\gamma_{J,t}x} f_t(x)dx + a_{2,2}\lambda_t^{\mathbb{Q}}) \times \int_{\mathbb{B}} x^2 f_t^{\mathbb{Q}}(x)dx$. For simplicity, further assume the intensity process is very persistent under both measures, $\frac{VRP_{t,T}^J}{T-t} \approx \lambda_t^{\mathbb{Q}} \times \int_{\mathbb{B}} x^2 f_t^{\mathbb{Q}}(x)dx - \lambda_t \times \int_{\mathbb{B}} x^2 f_t(x)dx$.

The implied variance IV_t quantified by VIX (CBOE), contains a bias from the jump process.[49] It measures

[49]Implied variance is commonly used in empirical asset pricing studies, see e.g. Bollerslev et al. (2009), Du and Kapadia (2012), among others.

the expected difference between the gross return and the log gross return under the risk neutral measure,

$$IV_{t,T} \equiv 2E_t^{\mathbb{Q}}[\int_t^T \frac{P_T}{P_t} - log\frac{P_T}{P_t}] \tag{A.15}$$

$$= E_t^{\mathbb{Q}}[CV_{t,T}] + 2E_t^{\mathbb{Q}} \int_t^T \int_{\mathbb{B}} (e^x - x - 1) v_s^{\mathbb{Q}}(dx)ds. \tag{A.16}$$

where P_t is the price for the aggregate market. Therefore,

$$E_t^{\mathbb{Q}}[\widehat{CV}_{t,T}] = IV_{t,T} - 2a_J\widehat{\lambda_t^{\mathbb{Q}}} \times \int_{\mathbb{B}}(e^x - x - 1)\widehat{f_t^{\mathbb{Q}}(x)}dx, \qquad \widehat{VRP}_{t,T}^{cv} = E_t^{\mathbb{Q}}[\widehat{CV}_{t,T}] - E_t[\widehat{CV}_{t,T}]. \tag{A.17}$$

where a_J is approximately $T - t$, $E_t[\widehat{CV}_{t,T}]$ is estimated together with EJX in equation (4.7) by using high frequency data in a HAR-VAR Kalman filter approach (Appendix C). To construct the volatility part of the equity risk premium, a parametric calibration is needed besides $\widehat{VRP}_{t,T}^{cv}$.

A.3 Implied Consumption

Based on this setup, the implied log consumption takes the following expression,

$$\begin{aligned} dlnC_t =& -\Psi\delta dt - \frac{\Psi}{\theta}(dlnM_t + (\theta - 1)lnR_{c,t}) \\ =& \left(-\Psi\delta + \frac{\Psi}{\theta}\left(m_t + r_{f,t} + (\theta - 1)[a_{c,t} - 0.5(\sigma_c^2 + \varphi_c^2 q_t) - \int_{\mathbb{B}}(e^{\frac{\gamma_{J,t}}{\gamma}x} - 1)J(dt, dx)]\right)\right)dt \\ &+ \sigma_c dW_{c^\perp,t} - (\varphi_c + \frac{\Psi}{\theta}\phi_q)\sqrt{q_t}dW_{q,t} + \int_{\mathbb{B}}\left[\frac{\gamma_{J,t}}{\gamma}x - \phi_{\lambda,t}\frac{\Psi}{\theta}\right]J(dt, dx) - \frac{\Psi}{\theta}\phi_f\sqrt{r_{f_t}}dW_{f,t} - \varphi_{A_\lambda}dW_{A_{\lambda,t},t}. \end{aligned} \tag{A.18}$$

The shock structure shows how consumption is co-moving with different sources of risk. The first shock component represents the endowment risk, which is a one-to-one mapping with the total wealth return. The next component says that, if Ψ(IES) is larger than 1 ($\theta < 0$), then when volatility uncertainty increases, consumption growth decreases (since $\phi_q < 0$). If Ψ(IES) is smaller than 1 ($\theta > 0$), to ensure the same relation, the parameter space for Ψ should be more restricted, $1 > \Psi > 1 - \varphi_c(1 - \gamma)/\phi_q$.

The third component captures the large discontinuous movement in the economy. Since the intensity premium is positive $\phi_{\lambda,t} > 0$,[50] it requires $\Psi > 1$ to ensure the consumption is less affected by left-jumps than the total wealth return. When $\Psi > 1$, the fourth component suggests that a positive monetary policy shock coincides with a decrease in consumption growth ($\phi_f < 0$). Lastly, regardless of the choice of Ψ(IES), a positive shock to the intensity risk premium ($\phi_{\lambda,t} > 0$) slows down the consumption growth rate.

[50] This is based on the estimation of $\phi_{\lambda,t}$ in section 5.

Note that since $0.5\frac{\Psi}{\theta}\gamma^2 + \frac{\Psi}{\theta}(\theta-1)(\gamma-0.5) + 0.5 = 0.5\gamma(\Psi+1)$, by Ito's lemma, the geometric consumption growth can be expressed as follows,

$$\begin{aligned}\frac{dC_t}{C_{t^-}} =& \left(-\Psi\delta + \left(0.5\frac{\Psi}{\theta}(\frac{\Psi}{\theta}+1)\phi_f^2 + \Psi\right)r_{f,t} + 0.5\frac{\Psi}{\theta}(\frac{\Psi}{\theta}+1)\phi_{A_\lambda}^2\right)dt \\ &+ \left(0.5\gamma(1+\Psi)\sigma_c^2 + \left(0.5\frac{\Psi}{\theta}(\frac{\Psi}{\theta}+1)\phi_q^2 + 0.5\gamma(1+\Psi)\varphi_c^2 + (\frac{\Psi}{\theta}+1)\varphi_c\phi_q\right)q_t\right)dt \\ &- (1-\frac{\Psi\gamma}{\theta})\int_{\mathbb{B}}(e^{\frac{\gamma_{J,t}}{\gamma}x}-1)v_t^{\mathbb{Q}}(x)dx + \frac{\Psi}{\theta}\int_{\mathbb{B}}(1-e^{\gamma\frac{\gamma_{J,t}}{\gamma}x-\phi_{\lambda,t}})v_t^{\mathbb{Q}}(x)dx \\ &+ \int_{\mathbb{B}}(e^{\frac{\gamma_{J,t}}{\gamma}x-A_{\lambda,t}\varphi_\lambda}-1)J(dt,dx) + \sigma_c dW_{c^\perp,t} - [\varphi_c + \frac{\Psi}{\theta}\phi_q]\sqrt{q_t}dW_{q,t} - \frac{\Psi}{\theta}\phi_f\sqrt{r_{f_t}}dW_{f,t} - \varphi_{A_\lambda}dW_{A_{\lambda,t},t}. \quad \text{(A.19)}\end{aligned}$$

with implied unconditional mean,

$$\begin{aligned}E\int_t^{t+\Delta T}\frac{dC_t}{C_{t^-}} =& -\Delta T\Psi\delta + E\int_t^{t+\Delta T}\left(0.5\frac{\Psi}{\theta}(\frac{\Psi}{\theta}+1)\phi_f^2 + \Psi\right)r_{f,s}ds + 0.5\frac{\Psi}{\theta}(\frac{\Psi}{\theta}+1)\phi_{A_\lambda}^2\Delta T \\ &+ 0.5\gamma(1+\Psi)\sigma_c^2\Delta T + \left(0.5\frac{\Psi}{\theta}(\frac{\Psi}{\theta}+1)\phi_q^2 + 0.5\gamma(1+\Psi)\varphi_c^2 + (\frac{\Psi}{\theta}+1)\varphi_c\phi_q\right)E\int_t^{t+\Delta T}q_s ds \\ &+ E\int_t^{t+\Delta T}\left[\int_{\mathbb{B}}(e^{\frac{\gamma_{J,t}}{\gamma}x-A_{\lambda,t}\varphi_\lambda}-1)v_s(x)dx - (1-\frac{\Psi\gamma}{\theta})\int_{\mathbb{B}}(e^{\frac{\gamma_{J,t}}{\gamma}x}-1)v_s^{\mathbb{Q}}(x)dx + \frac{\Psi}{\theta}\int_{\mathbb{B}}(1-e^{\gamma_{J,t}x-\phi_{\lambda,t}})v_s^{\mathbb{Q}}(x)dx\right].\end{aligned}$$

and a quadratic variance,

$$QV_{t,T} = \int_t^T\int_{\mathbb{B}}\left(\frac{\gamma_{J,t}}{\gamma}x - A_{\lambda,t}\varphi_\lambda\right)^2 v_t(x)dx + \sigma_c^2\Delta T + \int_t^T(\varphi_c + \frac{\Psi}{\theta}\phi_q)^2 q_s ds + \int_t^T\frac{\Psi^2}{\theta^2}\phi_f^2 r_{f,s}ds + \frac{\Psi^2}{\theta^2}\phi_{A_\lambda}^2\Delta T.$$

B Option Data Cleaning Rule

The cleaning filter for options are in line with the option literature. I first drop those observations with non-positive bid, and those with non-decreasing mid-quote as the moneyness goes deeper, unless the subsequent one has a larger volume. Future price F_t in equation (4.1) is constructed from a no arbitrage condition with spot price, dividend yield and zero-coupon rate.

Table [B.1] summarizes the number and trading volume of options per-month for the full sample. The number of options in each moneyness bin is very similar between the fixed moneyness and the floating moneyness. On average, the sample size of puts ($\log(\frac{K}{F}) < -2e^{\sigma_t^{ATM}\sqrt{\tau_t}}$) is three times larger than that of calls ($\log(\frac{K}{F}) > 1.75e^{\sigma_t^{ATM}\sqrt{\tau_t}}$). The associated trading volumes for these puts are ten times larger than calls.

Table [B.2] summarizes the number and the trading volume of options per-month for the data before the financial crisis. The number of options in each moneyness bin is smaller than the full sample average. The associated trading volumes for both puts ($\log(\frac{K}{F}) < -2e^{\sigma_t^{ATM}\sqrt{\tau_t}}$) and calls ($\log(\frac{K}{F}) > 1.75e^{\sigma_t^{ATM}\sqrt{\tau_t}}$) are largely reduced.

Figure [B.1] illustrates the estimation for the jump shape parameters $\alpha_t^{\mathbb{Q}\pm}$. The top (bottom) panel plots the log jump tails in equation (4.1) over the log moneyness space in October 2006 (October 1998). Compared with a calm period (October 2006), options in October 1998 obviously display a fatter tail in the strike dimension (smaller decay rate), signaling a lower $\alpha_t^{\mathbb{Q}\pm}$, and all together reflecting the temporal variation in the jump shape parameters.

Table B.1 Summary Statistics for the Options Data

This table summarizes the number and trading volume of out-of-money options each month for each moneyness range. The options data spans from 04Jan1996 to 30Dec2011 for a total of 4027 trading days. σ_t^{ATM} denotes at-the-money Black-Scholes (annualized) implied volatility on day t.

Fixed Moneyness

$\frac{K_t}{F_t}$	< 0.90	$(0.9, 0.925)$	$(1.025, 1.075)$	> 1.075
Number	278.35	61.15	76.92	123.51
Volume	303855	147188	187565	53103

Floating Moneyness

$\frac{log(K_t/F_t)}{\sigma_t^{ATM}\sqrt{\tau_t}}$	< -3	$(-3, -2.0)$	$(1, 1.75)$	> 1.75
Number	258.24	40.59	66.57	85.61
Volume	246961	64256	115984	21250

Table B.2 Summary Statistics for the Options Data— Subsample

This table summarizes the number and trading volume of out-of-money options per-month in each moneyness range. Our option data span from 04Jan1996 to 30Dec2007, a total of 4027 trading days. σ_t^{ATM} denotes at-the-money Black-Scholes (annualized) implied volatility on day t.

Fixed Moneyness

$\frac{K_t}{F_t}$	< 0.90	$(0.9, 0.925)$	$(1.025, 1.075)$	> 1.075
Number	159.61	53.70	28.56	108.71
Volume	144320	116711	103190	7584

Floating Moneyness

$\frac{log(K_t/F_t)}{\sigma_t^{ATM}\sqrt{\tau_t}}$	< -3	$(-3, -2.0)$	$(1, 1.75)$	> 1.75
Number	172.17	31.99	36.01	67.61
Volume	175762	34109	64237	7059

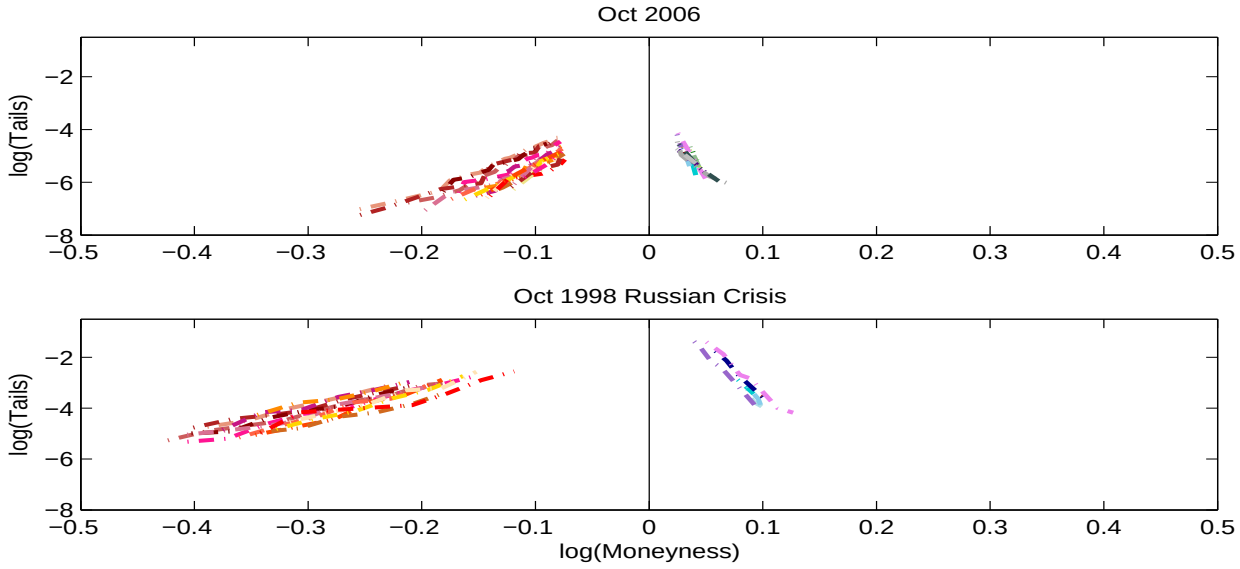

Figure B.1 Option Tails and Moneyness — An Example

This figure plots the log jump tails in equation (4.1) vs log moneyness for October 2006 (Top) and October 1998 (Bottom) as two examples. Puts are on the left and calls on the right with cutoff $k^{*-} = -2e^{\sigma_t^{ATM}\sqrt{\tau_t}}$ and $k^{*+} = 1.75e^{\sigma_t^{ATM}\sqrt{\tau_t}}$.

C Estimation of Tail Behavior Under $\mathbb{P}$

Literatures show that the 5-minutes intra-day return can non-parametrically quantify the continuous variation (CV), the jump variation (JV) and the jump tail index (JX). Thus, the unit time interval is set to be 5-minutes, n_0 is the close-open time length. Over one trading day $[t+n_0,\ \ t+n_0+n]$ where n=77, we have the following empirical measures for daily return variation,

$$ICV_{t+n_0,t+n_0+n} = \sum_{j=1}^{n} (\Delta_{t,j} f)^2 1_{|\Delta_{t,j} f| <= \omega_{j,t}} \xrightarrow{p} CV_{t+n_0,t+n_0+n}, \tag{C.1}$$

$$IRJV_{t+n_0,t+n_0+n} = \sum_{j=1}^{n} (\Delta_{t,j} f)^2 1_{[\Delta_{t,j} f] > \omega_{j,t}} \xrightarrow{p} JV^{+}_{t+n_0,t+n_0+n}, \tag{C.2}$$

$$ILJV_{t+n_0,t+n_0+n} = \sum_{j=1}^{n} (\Delta_{t,j} f)^2 1_{[\Delta_{t,j} f] < -\omega_{j,t}} \xrightarrow{p} JV^{-}_{t+n_0,t+n_0+n}, \tag{C.3}$$

$$IRJX_{t+n_0,t+n_0+n} = \sum_{j=1}^{n} e^{\Delta_{t,j} f} - e^{0.6/100} 1_{[\Delta_{t,j} f] > 0.6/100} \xrightarrow{p} JX^{+}_{t+n_0,t+n_0+n}, \tag{C.4}$$

$$ILJV_{t+n_0,t+n_0+n} = \sum_{j=1}^{n} e^{\Delta_{t,j} f} - e^{-0.6/100} 1_{[\Delta_{t,j} f] < -0.6/100} \xrightarrow{p} JX^{-}_{t+n_0,t+n_0+n}. \tag{C.5}$$

where f is the logarithm of the future price, $\Delta_{t,j} f = f_{t+n_0+j} - f_{t+n_0+j-1}$. The idea is to find a sufficiently large threshold $\omega_{j,t}$ to filter out price changes that are too large to be normally distributed. I then use a time-of-day factor to account for the different threshold choices at different times in a day. Formally,

$$TOD_j = \frac{\sum_{m=0}^{N} (\Delta_{m(n_0+n),j} f)^2 1_{|\Delta_{m(n_0+n),j} f| <= \bar{\omega}}}{\sum_{m=0}^{N} 1_{|\Delta_{m(n_0+n),j} f| <= \bar{\omega}}} \Big/ \frac{\sum_{m=0}^{N} \sum_{j=1}^{n} (\Delta_{m(n0+n),j} f)^2}{\sum_{m=0}^{N} \sum_{j=1}^{n} 1_{|\Delta_{m(n_0+n),j} f| <= \bar{\omega}}}. \tag{C.6}$$

where $\bar{\omega} = 3\sqrt{\pi/2}\sqrt{\frac{1}{N}\sum_{m=0}^{N}\sum_{j=1}^{n-1} |\Delta_{m(n0+n),j} f||\Delta_{m(n0+n),j+1} f|}$ and $\omega_{j,t} = 3(\frac{1}{n})^{0.49}\sqrt{ICV_{t-n,t}} TOD_j$. The time of day factor TOD_j is the ratio of the average continuous variation at j^{th} 5-min trading spot across different trading days (based on $\bar{\omega}$) and the average continuous variation across both different trading spots and trading days. In Figure C.1, TOD_j has a U shape pattern over NYSE trading hours, with separate end effects for the futures before and after the cash market opens.[51] As a result, the threshold $\omega_{j,t}$ depends on both the previous day's continuous variation and the time-of-day factor.

Based on the threshold $\omega_{j,t}$, Table C.1 reports the number of detected jumps for the full sample (January 1990-December 2011) and the sub-sample (January 1990-December 2007). Among these detected jumps, I choose 0.6% as the cutoff for the medium-sized ones. In turn, 185/1534 (162/1110) are medium-sized

[51] See Bollerslev and Todorov (2011b) for TOD_j plot in Appendix B.

downward (upward) jumps over the 22 years sample period, among which 61/185 (51/162) are found in the last 4 years.

Figure [C.2] plots the number of upward and downward medium-sized jumps based on the cutoff 0.6%. As can be seen, jumps cluster during the early 90s' recession, 00s' dot com bubbles and 08-10 financial crisis. This roughly indicates that the jump intensity is path-dependent.

Figure [C.3] is the histogram plot for upward and downward medium-sized jumps based on the cutoff 0.6% for the full and sub-sample periods. This clearly indicates that there is a similar number of upward and downward medium-sized jumps regardless of the choice of the sample period.

Next, to quantify the expected continuous variations and the expected jump index, I put the above variables together with the overnight return square $OVER^2 = (f_{t+n_0} - f_t)^2$ in a daily vector $Y = [ICV,\ ILJV,\ IRJV,\ ILJX,\ IRJX,\ OVER^2]$, where

$$E_t Y_{t+n+n_0} = c_0 + c_1 Y_t + c_5 Y_{t-(n+n_0)*5} + c_{22} Y_{t-(n+n_0)*22}. \tag{C.7}$$

then I use the Kalman filter to calculate the monthly expectation $E_t \sum_{j=1}^{22} Y_{t+(n+n_0)j}$.

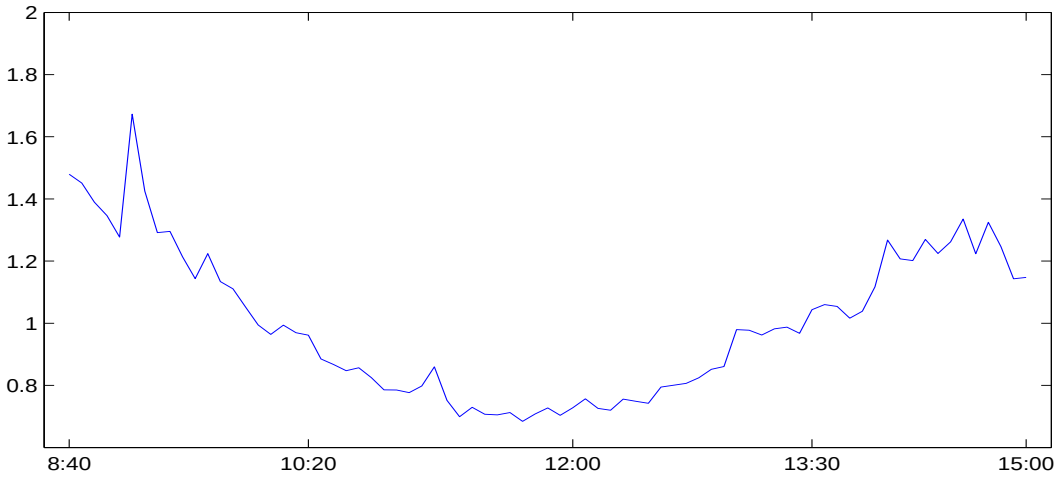

Figure C.1 Time-of-Day Factor

The estimates are based on 5-minute high-frequency S& P 500 futures data from 01Jan1990 through 30Dec2011.

Table C.1 Summary Statistics for the High-frequency Data

This table summarizes the total number and the average size of medium-sized jumps from 01Jan1990 to 30Dec2011.

Jan1990—Dec2011

cutoff	-0.6	$-\omega j,t$	$\omega j,t$	0.6
Number	185	1534	1110	162
Size	-0.9146			0.9788

Jan1990—Dec2007

cutoff	-0.6	$-\omega j,t$	$\omega j,t$	0.6
Number	124	1308	958	101
Size	-0.8586			0.8978

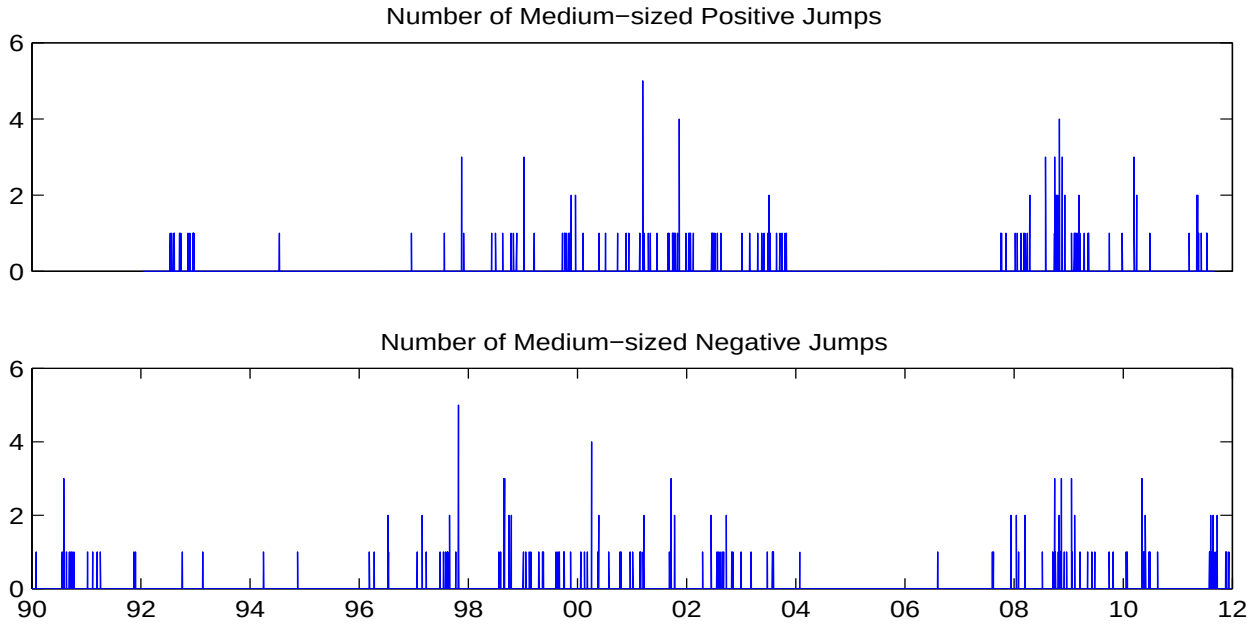

Figure C.2 Number of Medium-Size Jumps

This figure plots the number of positive and negative medium-sized jumps per day based on the cutoff 0.6% from 01Jan1990 to 30Dec2011 .

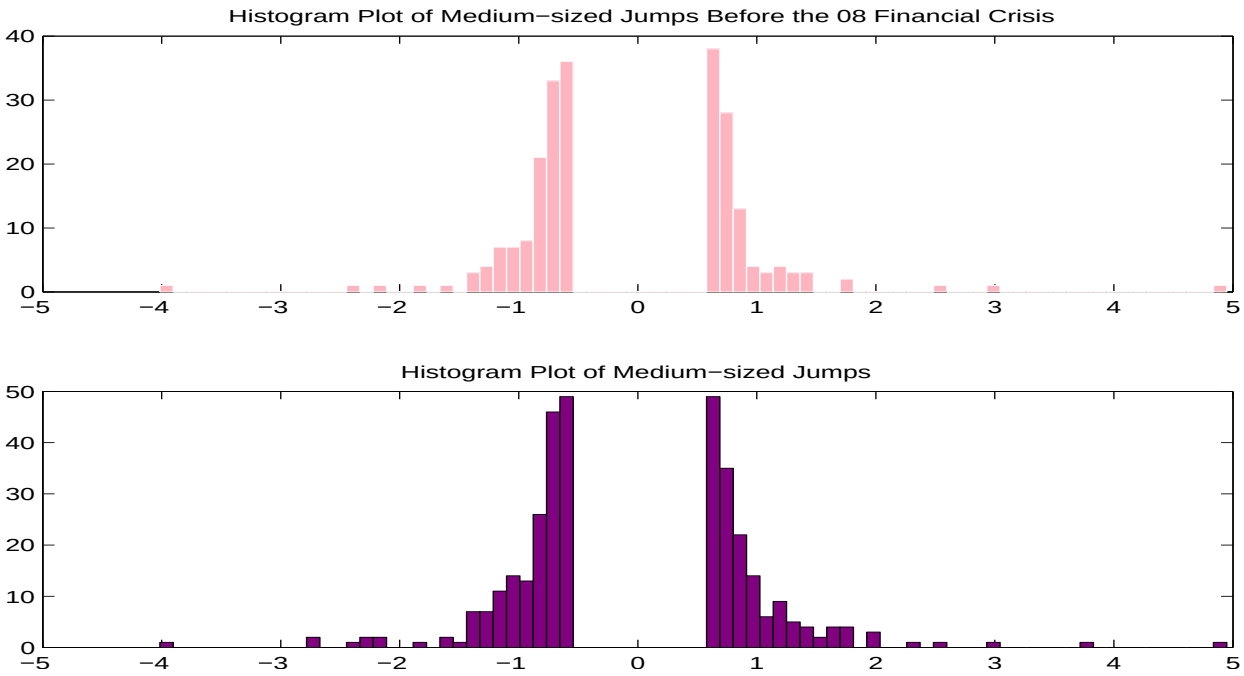

Figure C.3 Histogram Plot for Medium-Size Jumps

This figure plots the histogram of positive and negative medium-sized jumps per day based on the cutoff 0.6% from 01Jan1990 to 30Dec2007.

D Calibration Study

Besides estimations, it is also useful to conduct a simple calibration study to assess the model. In particular, the preference parameter γ, the dynamic parameters κ_q, φ_q and the leverage effect loading φ_c are four key ingredients to calculate the volatility price $\phi_q + \gamma\varphi_c$, and the sign and magnitude of φ_m will determine the direction of the pricing effects.

As presented in Table D.1, I first calibrate the continuous variation of the consumption growth as 0.0066^2 and the variation of the market returns as 0.048^2 on a monthly basis. Second, let the structural endowment risk $\sigma_c dW_{c\perp,t}$ account for four fifths of the total consumption variation (conditional correlation between total wealth return and volatility q_t is 0.4472). And at the same time, choose $\sigma_c dW_{c\perp,t} + \varphi_m \sqrt{q_t} dW_{q,t}$ to be three fifths of the total market return variation (conditional correlation between the market return and volatility q_t is -0.7746). Based on these constraints, the only free parameters left are the leverage effect parameter φ_m, κ_q and φ_q. Both the unconditional mean and the AC1 of continuous part of the variance risk premium (VRP^{cv}) match closely with that of the data, see Table 5.1. The equity risk premium of the S&P500 is about 4%, slightly lower than the observed. As such, the volatility price coefficient $\phi_q + \gamma\varphi_c = 0.0160$, the volatility part of equity risk premium $ERPV = \gamma\sigma_c^2 + \varphi_m(\phi_q + \gamma\varphi_c)q_t = 4 \times \frac{4}{5} 0.0066^2 + 0.1443(VRP_t^{cv} - 0.51)$ on a monthly basis, which on average accounts for 0.5462% of equity risk premium per-year.

Figure [D.1] plots the risk premium attributed to the volatility factor q_t. For a fixed risk aversion parameter, as the leverage effect increases from 0.4472 to 0.7746, the volatility risk premium increases accordingly. When the risk aversion becomes larger, all associated risk premia become larger regardless of the leverage effect level.

Table D.1 Partial Model Calibration

This table reports the model calibration for volatility pricing. The parameters σ_c^2, φ_c^2 and φ_m^2 are calibrated in monthly frequency, volatility dynamic parameters in 5-minutes frequency, implied unconditional mean for the continuous part of VRP_t^{cv} and S&P500 returns are in annualized percentage form.

Preference	γ		
	4		
Volatility	σ_c^2	$\varphi_c^2\mu_q$	$\varphi_m^2\mu_q$
	$\frac{4}{5}0.0066^2$	$\frac{1}{5}0.0066^2$	$\frac{3}{5}0.048^2$-σ_c^2
	μ_q	κ_q	φ_q
	$3.17e-4$	$3.81e-4$	0.0714
Implied Condition	$c_{VRP^{cv}}$	$\phi_q+\gamma\varphi_c$	
	0.2066	0.0160	
Implied Moments	E(VRP^{cv})	AC1(VRP_t)	E(r_{SP500})
	2.05	0.31	8.04

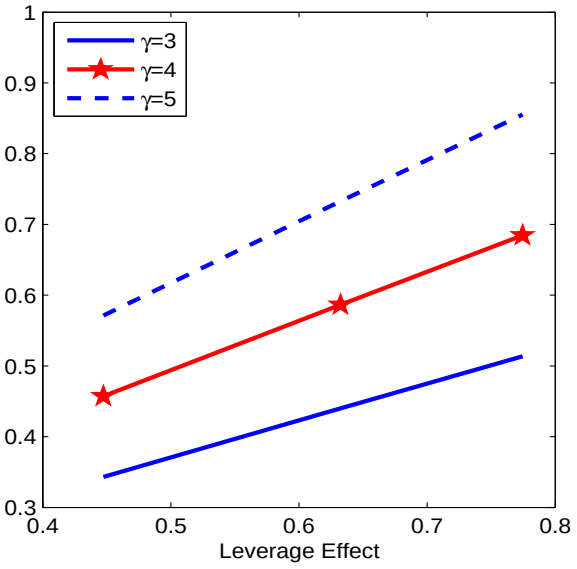

Figure D.1 The Mean of the Volatility Risk Premium

This figure is the analytical plot based on the calibration results in Table D.1. The starred line shows the magnitude of the volatility price $\gamma\sigma_c^2+\varphi_m(\gamma\varphi_c+\phi_q)\mu_q$ for different values of the variance ratio $w=\frac{\sigma_c^2+\varphi_m^2\mu_q}{\sigma_c^2+\varphi_m^2\mu_q+\sigma_m^2}$ when preference parameter $\gamma=4$; the dashed-dotted line for $\gamma=3$ and the solid line for $\gamma=5$.

E Return Predictability Studies

Table E.1 One Month Ahead Return Prediction

This table presents results for the aggregate market and the portfolio returns prediction studies at the one-month horizon. The regression covariates are the diffusive risk premium $ERPV$ and either the deeper tail of the jump risk premium $ERPJ(VIX)$ (e.g., for portfolio SMB, let $X_t = [ERPJ_{SMB}(VIX),\ ERPV_{SMB}]$) or the deeper tail of the left-jump risk premium $ERPJ^{-}(VIX)$ (i.e. for portfolio SMB, use $X_t = [ERPJ^{-}_{SMB}(VIX),\ ERPV_{SMB}]$). The sample ranges from January 1996 to December 2011.

	MRK		SMB		HML		WML	
Constant	-1.13	-0.59	1.38	1.91	1.73	2.01	2.69	1.80
std	(0.91)	(0.71)	(0.86)	(0.62)	(1.04)	(0.90)	(0.79)	(0.59)
ERPJ(VIX)		3.41		20.46		20.65		10.70
std		(1.31)		(6.17)		(8.45)		(10.72)
ERP$J^{-}(VIX)$	4.51		13.79		16.92		21.71	
std	(1.79)		(7.28)		(9.22)		(12.47)	
ERPV	-2.68	-2.54	-8.94	-10.29	-9.44	-10.69	-1.91	3.18
std	(1.18)	(1.09)	(5.98)	(6.17)	(3.94)	(3.64)	(6.05)	(5.42)
R^2	3.59	2.43	3.06	7.07	2.30	3.31	7.50	4.54
Adjusted R^2	2.58	1.41	2.04	6.10	1.27	2.30	6.53	3.54

Table E.2 Two Months Ahead Return Prediction

This table presents results for the aggregate market and the portfolio returns prediction studies at two-month horizons. The regressions are based on the deeper tail of the jump risk premium $ERPJ(VIX)$ and diffusive risk premium $ERPV$ (for portfolio SMB, use $X_t = [ERPJ_{SMB}(VIX),\ ERPV_{SMB}]$, etc.), and the deeper tail of the left-jump risk premium $ERPJ^{-}(VIX)$ and diffusive risk premium $ERPV$ (for portfolio SMB, use $X_t = [ERPJ^{-}_{SMB}(VIX),\ ERPV_{SMB}]$, etc.). The data sample ranges from January 1996 to December 2011.

	MRK		SMB		HML		WML	
Constant	-1.57	-1.42	2.28	2.72	3.90	3.93	5.89	3.88
std	(1.35)	(1.40)	(1.05)	(0.98)	(1.84)	(1.73)	(1.55)	(1.28)
ERPJ(VIX)		7.52		27.75		40.42		43.24
std		(2.31)		(8.01)		(15.50)		(23.63)
ERP$J^{-}(VIX)$	7.36		21.17		38.68		61.50	
std	(2.35)		(8.98)		(16.19)		(26.42)	
ERPV	-5.44	-5.56	-12.55	-14.02	-28.42	-28.80	-23.21	-15.14
std	(2.23)	(2.16)	(9.45)	(10.11)	(6.87)	(6.39)	(12.56)	(11.92)
R^2	5.76	6.17	2.94	5.55	6.55	6.97	18.84	14.39
Adjusted R^2	4.77	5.18	1.92	4.56	5.57	5.99	17.99	13.49

Table E.3 Three Months Ahead Return Prediction

This table presents results for the aggregate market and the portfolio returns prediction studies at three-month horizons. The regressions are based on the deeper tail of the jump risk premium $ERPJ(VIX)$ and diffusive risk premium $ERPV$ (for portfolio SMB, use $X_t = [ERPJ_{SMB}(VIX),\ ERPV_{SMB}]$, etc.), and the deeper tail of the left-jump risk premium $ERPJ^{-}(VIX)$ and diffusive risk premium $ERPV$ (for portfolio SMB, use $X_t = [ERPJ^{-}_{SMB}(VIX),\ ERPV_{SMB}]$, etc.). The data sample ranges from January 1996 to December 2011.

	MRK		SMB		HML		WML	
Constant	-3.70	-2.55	2.40	2.71	4.96	5.43	8.63	5.89
std	(2.08)	(2.04)	(1.25)	(1.23)	(2.09)	(2.04)	(2.21)	(1.81)
ERPJ(VIX)		10.76		31.11		54.54		51.70
std		(2.99)		(10.37)		(17.00)		(30.44)
$ERPJ^{-}(VIX)$	12.79		24.89		47.44		78.25	
std	(3.32)		(11.29)		(16.39)		(35.85)	
ERPV	-4.71	-4.52	-21.55	-23.26	-17.52	-19.80	-14.27	-2.40
std	(2.49)	(2.34)	(13.23)	(13.94)	(6.96)	(7.01)	(15.10)	(12.91)
R^2	8.84	6.53	3.40	5.20	6.14	8.01	27.83	20.33
Adjusted R^2	7.88	5.54	2.37	4.20	5.15	7.03	27.07	19.49

Table E.4 Four Months Ahead Return Prediction

This table presents results for the aggregate market and the portfolio returns prediction studies at four-month horizons. The regressions are based on the deeper tail of the jump risk premium $ERPJ(VIX)$ and diffusive risk premium $ERPV$ (for portfolio SMB, use $X_t = [ERPJ_{SMB}(VIX),\ ERPV_{SMB}]$, etc.), and the deeper tail of the left-jump risk premium $ERPJ^{-}(VIX)$ and diffusive risk premium $ERPV$ (for portfolio SMB, use $X_t = [ERPJ^{-}_{SMB}(VIX),\ ERPV_{SMB}]$, etc.). The data sample ranges from January 1996 to December 2011.

	MRK		SMB		HML		WML	
Constant	-4.85	-3.16	1.56	1.94	4.75	5.69	10.82	7.82
std	(2.73)	(2.52)	(1.53)	(1.54)	(2.25)	(2.17)	(2.62)	(2.26)
ERPJ(VIX)		11.15		31.27		54.71		48.25
std		(3.29)		(14.76)		(17.79)		(31.88)
$ERPJ^{-}(VIX)$	14.51		24.43		42.73		80.59	
std	(3.89)		(14.44)		(16.52)		(36.19)	
ERPV	-0.24	0.18	-38.04	-39.77	3.39	-0.67	6.45	21.14
std	(2.68)	(2.63)	(14.59)	(15.15)	(7.09)	(7.24)	(14.73)	(13.15)
R^2	8.28	5.11	5.03	6.55	5.21	7.56	36.54	28.75
Adjusted R^2	7.31	4.10	4.02	5.55	4.20	6.58	35.87	27.99

Table E.5 Five Months Ahead Return Prediction

This table presents results for the aggregate market and the portfolio returns prediction studies at five-month horizons. The regressions are based on the deeper tail of the jump risk premium $ERPJ(VIX)$ and diffusive risk premium $ERPV$ (for portfolio SMB, use $X_t = [ERPJ_{SMB}(VIX),\ ERPV_{SMB}]$, etc.), and the deeper tail of the left-jump risk premium $ERPJ^{-}(VIX)$ and diffusive risk premium $ERPV$ (for portfolio SMB, use $X_t = [ERPJ^{-}_{SMB}(VIX),\ ERPV_{SMB}]$, etc.). The data sample ranges from January 1996 to December 2011.

	MRK		SMB		HML		WML	
Constant	-4.02	-2.67	0.99	2.04	6.89	7.58	12.30	9.77
std	(3.29)	(3.20)	(1.71)	(1.64)	(2.87)	(2.77)	(2.96)	(2.81)
ERPJ(VIX)		10.40		39.03		73.60		60.38
std		(4.82)		(17.65)		(22.08)		(41.86)
$ERPJ^{-}(VIX)$	12.91		25.26		63.37		78.97	
std	(4.86)		(17.68)		(21.24)		(41.36)	
ERPV	0.76	1.02	-51.58	-54.80	-1.00	-4.31	18.99	26.88
std	(3.18)	(3.18)	(16.62)	(18.08)	(9.78)	(10.03)	(18.04)	(19.12)
R^2	5.07	3.40	6.68	9.11	7.46	9.40	34.87	33.00
Adjusted R^2	4.05	2.37	5.68	8.14	6.47	8.43	34.17	32.28

Table E.6 Six Months Ahead Return Prediction

This table presents results for the aggregate market and the portfolio returns prediction studies at six-month horizons. The regressions are based on the deeper tail of the jump risk premium $ERPJ(VIX)$ and diffusive risk premium $ERPV$ (for portfolio SMB, use $X_t = [ERPJ_{SMB}(VIX),\ ERPV_{SMB}]$, etc.), and the deeper tail of the left-jump risk premium $ERPJ^{-}(VIX)$ and diffusive risk premium $ERPV$ (for portfolio SMB, use $X_t = [ERPJ^{-}_{SMB}(VIX),\ ERPV_{SMB}]$, etc.). The data sample ranges from January 1996 to December 2011.

	MRK		SMB		HML		WML	
Constant	-4.37	-3.68	1.66	2.65	8.72	9.05	13.85	11.61
std	(3.88)	(4.13)	(1.95)	(1.80)	(3.67)	(3.53)	(3.36)	(3.43)
ERPJ(VIX)		13.91		54.17		87.61		82.43
std		(6.24)		(19.48)		(26.16)		(50.51)
$ERPJ^{-}(VIX)$	14.48		39.04		80.50		86.63	
std	(5.57)		(19.85)		(26.41)		(46.38)	
ERPV	0.79	0.68	-73.13	-76.68	-6.85	-8.92	19.13	19.87
std	(3.79)	(3.84)	(22.31)	(24.79)	(10.95)	(11.42)	(20.73)	(23.43)
R^2	5.05	4.66	11.39	14.72	8.97	10.20	31.75	34.88
Adjusted R^2	4.03	3.64	10.44	13.80	7.99	9.24	31.02	34.18

References

Aït-Sahalia, Y.; J. Cacho-Diaz; and R. Laeven. "Modeling Financial Contagion Using Mutually Exciting Jump Processes." (2013) Working paper, Princeton University, University of Amsterdam and CentER.

Aït-Sahalia, Y.; M. Karaman; and L. Mancini. "The Term Structure of Variance Swaps, Risk Premia and the Expectation Hypothesis." (2012) Working paper, Princeton University and EPFL.

Bakshi, G.; C. Cao; and Z. Chen. "Empirical Performance of Alternative Option Pricing Models." *Journal of Finance* 52 (1997), 2003–2049.

Bansal, R., and A. Yaron. "Risks for the Long Run: A Potential Resolution of Asset Pricing Puzzles." *The Journal of Finance* 59 (2004), 1481–1509.

Barndorff-Nielsen, O., and N. Shephard. "Power and Bipower Variation with Stochastic Volatility and Jumps." *Journal of Financial Econometrics* 2 (2004), 1–37.

Bates, D. S. "Jumps and Stochastic Volatility: Exchange Rate Process Implicit in Deutsche Mark Options." *The Review of Financial Studies* 9 (1996), 69–107.

Bates, D. S. "Post-'87 Crash Fears in S&P 500 Future Options." *Journal of Econometrics* 94 (2000), 181–238.

Bollerslev, T.; J. Marrone; L. Xu; and H. Zhou. "Stock Return Predictability and Variance Risk Premia: Statistical Inference nd International Evidence." *Journal of Financial and Quantitative Analysis* (2011) forthcoming.

Bollerslev, T.; N. Sizova; and G. Tauchen. "Volatility in Equilibrium: Asymmetries and Dynamic Dependencies." *Review of Finance* 16 (2012), 31–80.

Bollerslev, T.; G. Tauchen; and H. Zhou. "Expected Stock Returns and Variance Risk Premia." *Review of Financial Studies* 22 (2009), 4463–4492.

Bollerslev, T., and V. Todorov. "Tails, Fears and Risk Premia." *Journal of Finance* 66 (2011b), 2165–2211.

Bollerslev, T., and V. Todorov. "Time-Varying Jump Tails." *Journal of Econometrics* (2013) forthcoming.

Broadie, M.; M. . Chernov; and M. Johannes. "Specification and Risk Premiums: The Information in S&P 500 Futures Options." *Journal of Finance* 62 (2007), 1453–1490.

Campbell, J. Y. "Intertemporal Asset Pricing Without Consumption Data." 83 (1993), 487–512.

Campbell, J. Y.; S. Giglio; C. Polk; and R. Turley. "An Intertemporal CAPM with Stochastic Volatility." (2013) working paper, Harvard University, University of Chicago and London School of Economics.

Campbell, J. Y., and R. J. Shiller. "Stock Prices, Earnings, and Expected Dividends." *Journal of Finance* 43 (1988), 661–676.

Carr, P., and L. Wu. "What Type of Process Underlies Options? A Simple Robust Test." *Journal of Finance* 58 (2003), 2581–2610.

Drechsler, I., and A. Yaron. "What's Vol Got to Do With It." *Review of Financial Studies* 24 (2011), 1–45.

Du, J., and N. Kapadia. "Tail and Volatility Indices from Option Prices." (2012) working paper, University of Massachusetts, Amherst.

Engsted, T.; T. Q. Pedersen; and C. Tanggaard. "The Log-Linear Return Approximation, Bubbles, and Predictability." *Journal of Financial and Quantitative Analysis* (2012) forthcoming.

Eraker, B. "Do Stock Prices and Volatility Jump? Reconciling Evidence from Spot and Option Prices." *Journal of Finance* (2004).

Eraker, B., and I. Shaliastovich. "An Equilibrium Guide to Designing Affine Pricing Models." *Mathematical Finance* 18 (2008), 519–543.

Galbraith, J. W., and S. Zernov. "Cricuit Breakers and the Tail Index of Equity Returns." *Journal of Financial Econometrics* 2 (2004), 109–129.

Hamidieh, K. "Estimating the Tail Shape Parameter from Option Prices." (2012) Working paper: California State University Fullerton.

Hawkes, A. "Spectra of some self-exciting and mutually exciting point processes." *Biometrica* 58 (1971b), 83–90.

Heston, S. "A Closed-Form Solution for Options with Stochastic Volatility with Applications to Bond and Currency Options." *Review of Financial Studies* 6 (1993), 327–343.

Jacod, J., and V. Todorov. "Do price and volatility jump together?" *Annals of Applied Probability* 20 (2010), 1425–1469.

Kelly, B. T. "Tail Risk and Asset Prices." (2011) Working paper, Booth School of Business, University of Chicago.

Kou, S., and H. Wang. "Option Pricing under a Double Exponential Jump Diffusion Model." *Management Science* 50 (2002), 1178–1192.

Li, J., and G. Zinna. "Variance Components, Term Structures of Variance Risk Premia, and Expected Asset Returns." (2013) Working paper, ESSEC Business School.

Maheu, J.; T. McCurdy; and X. Zhao. "Do jumps contribute to the dynamics of the equity premium?" *Journal of Financial Economics* (2013).

Pan, J. "The Jump-Risk Premia Implicit in Options: Evidence from an Integrated Time-Series Study." *Journal of Financial Economics* 63 (2002), 3–50.

Santa-Clara, P., and S. Yan. "Crashes, Volatility and the Equity Premium: Lessons from S&P 500 Options." *Review of Economics and Statistics* 92 (2010), 435–451.

Vilkov, G., and Y. Xiao. "Option-Implied Information and predictability of Extreme Returns." (2013) Working paper: Goethe University Frankfurt.

Wachter, J. A. "A Consumption-Based Model of the Term Structure of Interest Rates." *Journal of Financial Economics* 79 (2006), 365–399.